## **BC** RESEARCH ARTICLE



## N-glycan core tri-fucosylation requires Golgi α-mannosidase III activity that impacts nematode growth and behavior

Received for publication, August 12, 2024, and in revised form, October 4, 2024 Published, Papers in Press, October 29, 2024, https://doi.org/10.1016/j.jbc.2024.107944

Jonatan Kendler<sup>1</sup>, Florian Wöls², Saurabh Thapliyal³, Elsa Arcalis⁴, Hanna Gabriel¹, Sascha Kubitschek¹, Daniel Malzl<sup>2</sup>, Maria R. Strobl<sup>2</sup>, Dieter Palmberger<sup>2</sup>, Thomas Luber<sup>6</sup>, Carlo Unverzagt<sup>6</sup>, Katharina Paschinger<sup>2</sup>, Dominique A. Glauser<sup>3</sup>, lain B. H. Wilson<sup>2</sup>, and Shi Yan<sup>1,\*</sup>

From the <sup>1</sup>Institut für Parasitologie, Veterinärmedizinische Universität, Wien, Austria; <sup>2</sup>Department für Chemie, Universität für Bodenkultur, Wien, Austria; <sup>3</sup>Department of Biology, University of Fribourg, Fribourg, Switzerland; <sup>4</sup>Department für angewandte Genetik und Zellbiologie, Universität für Bodenkultur, Wien, Austria; <sup>5</sup>Department für Biotechnologie, Universität für Bodenkultur, Wien, Austria; <sup>6</sup>Bioorganic Chemistry, University of Bayreuth, Bayreuth, Germany

Reviewed by members of the JBC Editorial Board. Edited by Robert Haltiwanger

N-glycans with complex core chitobiose modifications are observed in various free-living and parasitic nematodes but are absent in mammals. Using Caenorhabditis elegans as a model, we demonstrated that the core *N*-acetylglucosamine (GlcNAc) residues are modified by three fucosyltransferases (FUTs), namely FUT-1, FUT-6, and FUT-8. Interestingly, FUT-6 can only fucosylate N-glycans lacking the α1,6-mannose upper arm, indicating that a specific α-mannosidase is required to generate substrates for subsequent FUT-6 activity. By analyzing the N-glycomes of aman-3 KOs using offline HPLC-MALDI-TOF MS/MS, we observed that the absence of aman-3 abolishes α1,3-fucosylation of the distal GlcNAc of N-glycans, which suggests that AMAN-3 is the relevant mannosidase on whose action FUT-6 depends. Enzymatic characterization of recombinant AMAN-3 and confocal microscopy studies using a knock-in strain (aman-3::eGFP) demonstrated a Golgi localization. In contrast to the classical Golgi α-mannosidase II (AMAN-2), AMAN-3 displayed a cobalt-dependent α1,6-mannosidase activity toward N-glycans. Using AMAN-3 and other C. elegans glycoenzymes, we were able to mimic nematode N-glycan biosynthesis in vitro by remodeling a fluorescein conjugated-glycan and generate a tri-fucosylated structure. In addition, using a high-content computer-assisted C. elegans analysis platform, we observed that aman-3 deficient worms display significant developmental delays, morphological, and behavioral alterations in comparison to the WT. Our data demonstrated that AMAN-3 is a Golgi α-mannosidase required for core fucosylation of the distal GlcNAc of N-glycans. This enzyme is essential for the formation of the unusual trifucosylated chitobiose modifications in nematodes, which may play important roles in nematode development and behavior.

Protein glycosylation is a ubiquitous and evolutionarily conserved posttranslational modification observed across diverse species. It exerts pleiotropic effects on many biological

phenomena under both physiological and pathophysiological conditions. As an important modulator of signaling, cell adhesion, and cell-cell interactions, protein glycosylation profoundly influences embryogenesis, tissue homeostasis, as well as cancer progression (1-3). The nervous system also relies on precise glycosylation for proper neuronal development and function (4). Moreover, glycoconjugates of pathogens are the major determinants that trigger immune responses, as they often possess ligands for innate immune recognition and promote production of anti-glycan antibodies (5, 6).

Caenorhabditis elegans has been used as a good model to study the glycosylation patterns conserved among parasitic species. In contrast to mammals, it has been shown that C. elegans can express complicated core modified N-glycan structures and a portion of these structural elements (glycoepitopes) can also be found in parasitic nematodes (7). Some nematode glycoepitopes are obviously immunogenic in mammals, for instance the anti-horseradish peroxidase epitope (core α1,3-fucose) is recognized by immunoglobulins (Igs) IgE and IgG antibodies of the host (8, 9).

Correct glycosylation of an antigen is considered, in addition to the protein backbone, an important factor for the antigenicity of parasite proteins. Therefore, identifying the correct glycoepitopes and glycan structures on the native glycoproteins and characterizing the glyco-enzymes involved in the biosynthesis are two major challenges for glycobiologists.

In our previous work, we have proven the function of the three fucosyltransferases (FUTs), which are involved in the biosynthesis of the highly fucosylated N-glycan core in C. elegans: FUT-1 and FUT-8, respectively, direct the \alpha1,3and α1,6-fucosylation of the proximal N-acetylglucosamine (GlcNAc) residue (10, 11), whereas FUT-6 is responsible for α1,3-fucosylation of the distal GlcNAc residue (summarized in Fig. 1) (12). Homologs of C. elegans FUT-8 have been well-studied in both vertebrates and invertebrates (11, 13, 14); enzymes with the same function as FUT-1 are characterized from plants and invertebrates (15), whereas FUT-6 (12) is a

<sup>\*</sup> For correspondence: Shi Yan, shi.yan@vetmeduni.ac.at.



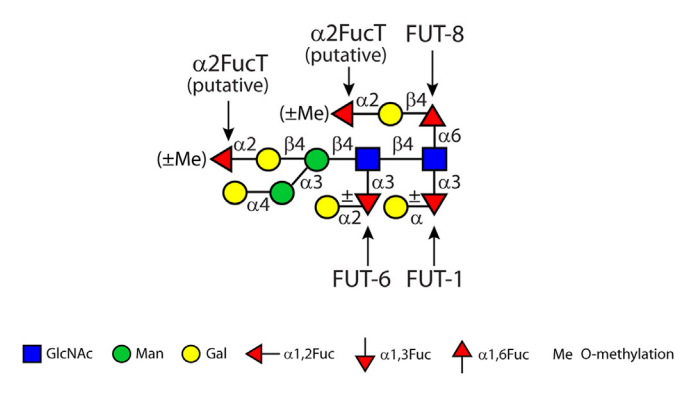


Figure 1. An illustration of fucose-rich glycans of the WT Caenorhabditis elegans using the Symbol Nomenclature for Glycans (SNFG) (49). Known fucosyltransferases (FUTs) as well as putative  $\alpha$ 1,2-fucosyltransferases ( $\alpha$ 2FucTs) responsible for fucosylation of the N-glycan core region with the specific glycosidic linkage are indicated with arrows.

unique core FUT occurring in some nematodes. It is noteworthy that FUT-6 displayed a strong bias against the presence of the  $\alpha$ 1,6-mannose residue (known as the "upper-arm") in contrast to the  $\alpha$ 1,3-mannose residue (known as the "lower-arm") of N-glycan structures as judged by the results of *in vitro* enzymatic assays (12); in other words, FUT-6 only fucosylated the structures lacking the  $\alpha$ 1,6-linked mannose. Analyzing the glycan structures from WT and *fut-6* deficient mutants as well as a double hexosaminidase mutant (*hex-2;hex-3*) yielded further evidence for this property of FUT-6 (16).

In addition to the core difucosylation of the proximal GlcNAc residue, distal GlcNAc fucosylation seems to be conserved in a number of nematode species, such as Pristionchus pacificus, Ascaris suum, Oesophagostomum dentatum, and Haemonchus contortus (16-19), probably due to the activity of FUT-6 orthologues, but are absent from filarial worms or Trichuris suis (9, 20). In the case of Haemonchus, a predicted glycosyltransferase (Genbank accession number: CDJ84058.1) possesses the highest homology to *C. elegans* FUT-6 in comparison to other FUT homologs. Consistent with the in vitro properties of FUT-6 (see above), detailed N-glycan structural analyses of these nematodes suggested the absence of the α1,6-mannose residue on the glycans which carry either solely an \$\alpha 1,3\$-linked fucose or a galactosylated fucose disaccharide unit on the distal GlcNAc. Presumably, the "upper arm" generates a steric hindrance which restricts the access of FUT-6 to the 3-OH position of the distal GlcNAc. These observations led to the assumption that a Golgi α1,6mannosidase activity must be essential for a proper biosynthesis of such structures prior to further processing by FUT-6 homologs.

There are three glycosyl hydrolase GH38 homologs in *C. elegans*: one lysosomal (AMAN-1), one classical Golgi mannosidase II (AMAN-2), and a hypothetical mannosidase (AMAN-3). In insects, enzymes with similarities to the latter (mannosidase III or ManIIb) have been characterized and shown to have Co(II)-dependent activities toward N-glycans (21, 22). In contrast to AMAN-2 that unequivocally impacts *C. elegans* N-glycan biosynthesis, it remained unclear if AMAN-3 can process N-glycoproteins despite its activity

toward an artificial substrate in the presence of Cobalt(II) chloride (23). By BLAST search using the extracellular domain of *C. elegans* AMAN-3,  $\alpha$ -mannosidase III homologs can also be found in *H. contortus* (CDJ83252.1) and *A. suum* (ERG79326.1) with 39% and 44% identity, respectively. Therefore, it is highly possible that in addition to FUT-1 and FUT-8 homologs, these nematodes also express  $\alpha$ -mannosidase III and FUT-6 homologs, which may sequentially act on N-glycans to create the highly fucosylated core structures found in these species.

In this study, we systematically investigated the enzymatic properties of the *C. elegans* AMAN-3 and proved its involvement in N-glycan biosynthesis. AMAN-3 deficiency not only impacts the core fucosylation patterns of nematode N-glycoproteins, but also alters animal development and results in behavioral changes.

#### Results

## $\alpha$ 1,6-specific mannosidase activity is lacking in aman-3 mutant worm lysates

In a previous study, we showed that the unpurified recombinant product of C. elegans F48C1.1 or aman-3 gene could degrade p-nitrophenyl-α-mannoside and potentially cause degradation of pyridylaminated Man<sub>5</sub>GlcNAc<sub>2</sub> (23). In order to confirm the Co(II)-dependent mannosidase activity of native AMAN-3, verify its sensitivity to the swainsonine inhibitor and better delineate its N-glycan substrate specificity, we conducted additional analyses to assess how a selected Nglycan (Man<sub>3</sub>GlcNAc<sub>2</sub>, 2-aminopyridine labelled MM structure [PA-MM] in Fig. 2) is processed by lysates from WT worms (N2), aman-3 loss-of-function mutants (tm5400), and hex-2;hex-3 mutants with deletions in two Golgi hexosaminidase genes (16). Noteworthily, the hex-2;hex-3 mutant is known to possess high amount of N-glycan structures missing the α1,6-mannose upper-arm, presumably due to a high α1,6specific mannosidase activity in this mutant. At approximately neutral pH, a removal of one mannose from PA-MM was observed with N2 and hex-2;hex-3 lysates (Fig. 2, D and F), but not for the *aman-3* lysate (Fig. 2, H and I); this is evidenced by the appearance of a new HPLC peak at 5.7 g.u. and confirmed by MALDI-TOF-MS (loss of 162 Da). Based on the observed mass change and the forward shift in elution time, the Man<sub>2-</sub> GlcNAc<sub>2</sub> product was identified Manα1,3-Man $\beta$ 1,4GlcNAc $\beta$ 1,4GlcNAc-PA (17, 24). We conclude that the aman-3 mutant lacked an Co(II)-dependent, swainsonineinhibitable α1,6-specific mannosidase activity.

#### N-glycomes of aman-3 deficient mutants

Many N-glycans in WT *C. elegans* lack the  $\alpha$ 1,6-mannose residue as well as a "lower arm"  $\beta$ 1,2-GlcNAc residue on the  $\alpha$ 1,3-mannose (25–27), whereas the *hex-2;hex-3* double mutant has high amounts of glycans lacking the  $\alpha$ 1,6-mannose, but presenting the nonreducing GlcNAc residue (16); on the other hand, the *bre-1* mutant lacks fucosylated glycans due to a mutation in the GDP-Man dehydratase gene (28). Therefore, considering the hypothesis that AMAN-3 was

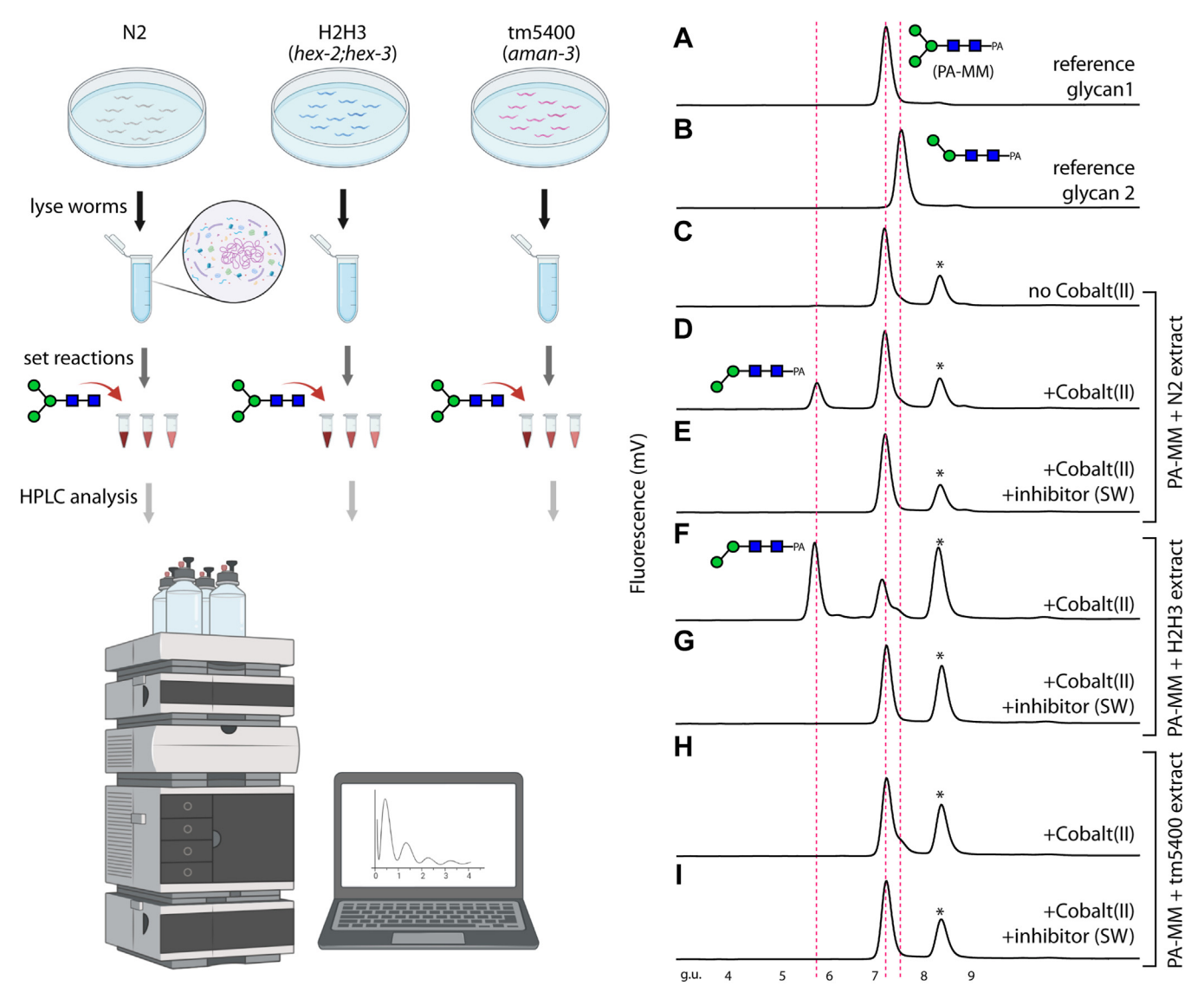


Figure 2. Detection of AMAN-3 activity in the crude extracts of different Caenorhabditis elegans strains. Worms were lysed to release native enzymes and clear supernatants were used to digest a pyridylamino-labeled N-glycan under various conditions; reaction mixtures were analyzed on reversed phase HPLC (left panel, created with BioRender.com). A selected N-glycan (A, PA-MM, 7.2 g.u.) was incubated with worm supernatants prepared from either the WT (N2; C-E), hex-2;hex-3 double KO (H2H3; F and G) or an aman-3 single KO (tm5400; H and I) with/without the presence of Cobalt (II) or Cobalt (II) plus swainsonine (SW). (B) shows the elution of a less improtant reference compound that was used to aid structural analysis. The presence of an early eluting product, missing the  $\alpha$ 1,6-linked mannose, on HPLC chromatograms (D and F) indicated the  $\alpha$ -mannosidase III activities. This cobalt (II)-dependent demannosylation was only observed when N2 or H2H3 extract was used but was absent when the tm5400 extract was used (H). Peaks marked with an asterisk contain nonglycan contaminants; g.u. is an abbreviation of glucose units. The peaks were all analyzed by MALDI-TOF MS and the major Co(II)dependent product at 5.7 g.u. shown to have a glycan of m/z 827 [M+H]<sup>+</sup> as compared to the substrate of m/z 989.

an α1,6-specific mannosidase that may impact fucosylation, we compared WT (N2), hex-2;hex-3 and bre-1 strains with an aman-3 mutant (tm5400) and a hex-2;hex-3;aman-3 triple mutant (cop1842). Distinct and major shifts in the PNGase Areleased N-glycome were observed for all mutants examined and up to three fucose residues were detected in the overall MALDI-TOF MS profile for the aman-3 mutant but only one fucose in the hex-2;hex-3;aman-3 triple mutant (Fig. 3), whereby the major N-glycans in these two strains were respectively, Hex<sub>5</sub>HexNAc<sub>2</sub>Fuc<sub>2-3</sub> and Hex<sub>4</sub>HexNAc<sub>3</sub>Fuc<sub>1</sub>. In line with a previous study (28), no fucosylated N-glycan was detected in the N-glycome of bre-1, which suggested the complete absence of core and antennal fucose in this mutant (Fig. 3B).

To investigate the N-glycomic changes more exactly, HPLC was performed on a fused core RP-amide column and fractions were individually subject to MALDI-TOF tandem mass spectrometry (MS/MS) (Fig. 4). The major glycan in the triple mutant (Hex<sub>4</sub>HexNAc<sub>3</sub>Fuc<sub>1</sub>; m/z 1500 as a pyridylaminated glycan) possessed a "GalFuc" motif, due to β1,4-galactosylation of the core α1,6-fucose by GALT-1 (29), resulting in a strong Y1 fragment at m/z 608 (Fig. 4B). The traces of glycans with two fucose residues were due to α1,2-fucosylation of the GalFuc (Y1 fragment at m/z 754), an epitope previously found in some FUT mutants (30). The high degree of substitution of the  $\alpha$ 1,3-mannose by the  $\beta$ 1,2-GlcNAc residue in the triple mutant is probably the reason for the lack of methylation or  $\alpha$ galactosylation of the  $\alpha$ 1,3-mannose as well as the absence of



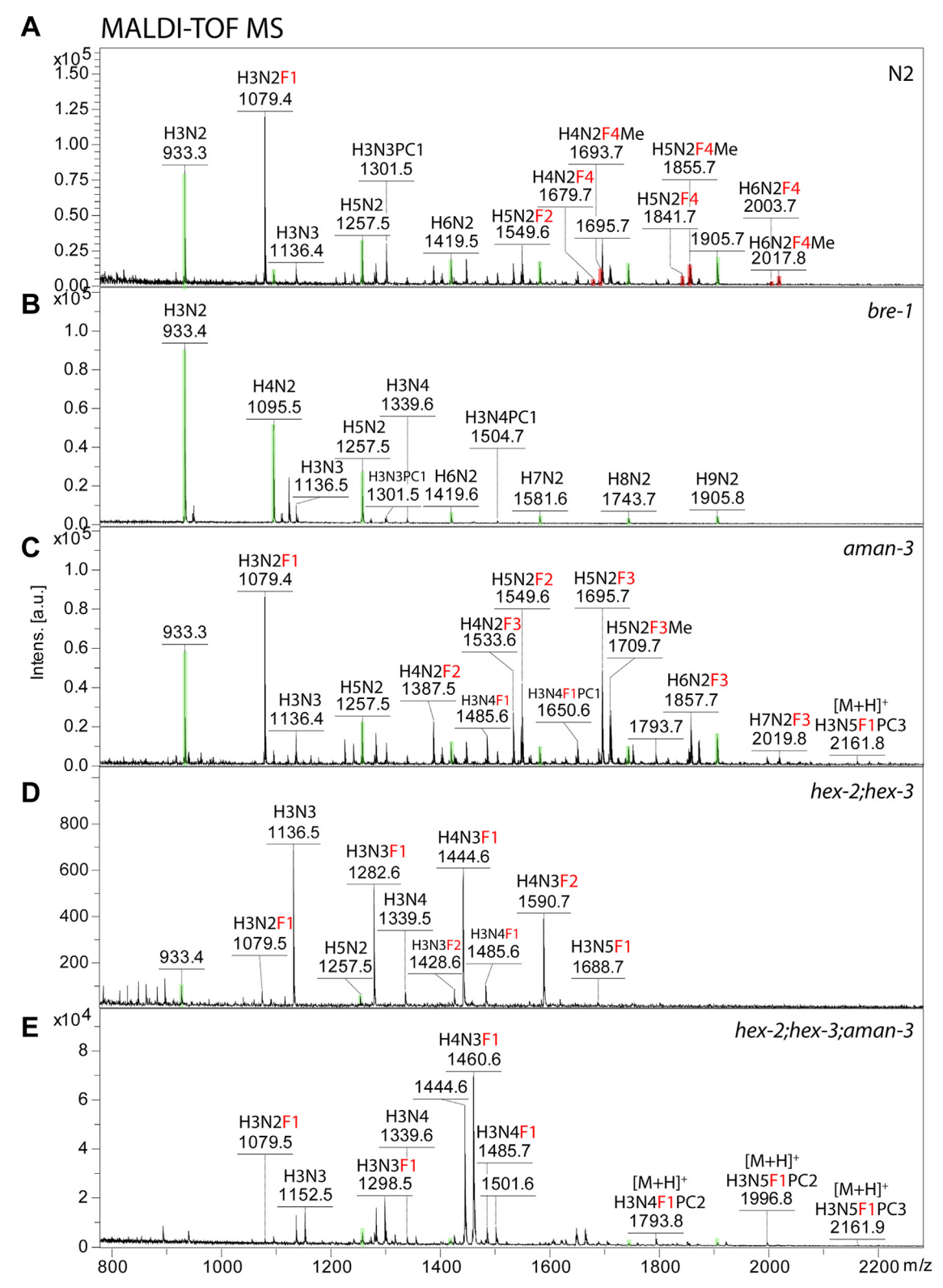


Figure 3. MALDI-TOF MS spectra of native N-glycans from the WT and KO strains. N-glycans released by PNGase A were subject to solid phase extraction and MS analysis. Most of the glycans present on the spectra are in  $[M+Na]^+$  and  $[M+K]^+$  forms except for PC-modified glycans detected partly in  $[M+H]^+$  forms. Peaks are annotated with m/z values and glycan compositions (H, hexose; N, N-acetyl-hexosamine; F, fucose, highlighted in red; Me, methyl group; PC, phosphorylcholine). Peaks indicating pauci- and oligo-mannosidic glycans are highlighted in green. In comparison to the N2 WT that possesses tetrafucosylated N-glycans (A), underfucosylation with maximal three fucoses is observed in aman-3 single mutant (C). In comparison to the H2H3 double mutant (D) (16), hex-2;hex-3;aman-3 triple knockout (E) possesses three major compositions ( $H_3-4N_3F_{0-1}$ ) and the difucosylated glycan  $H_4N_3F_2$  (m/z 1590) is absent on the spectrum (the fourth and fifth panels). Bre-1 (28) is a fucose-free mutant deficient in GDP-mannose 4,6-dehydratase (B). MS, mass spectrometry.

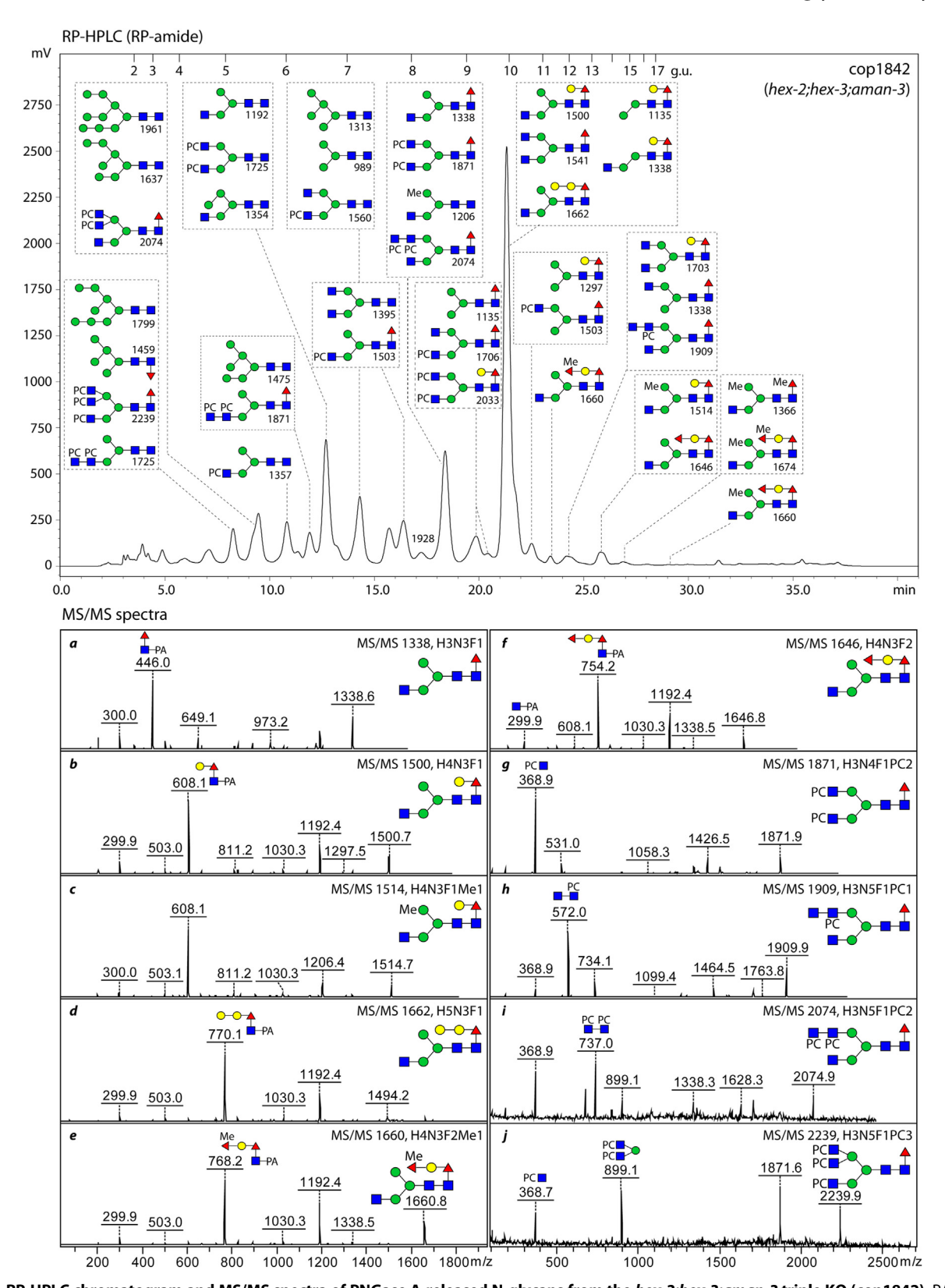


Figure 4. RP-HPLC chromatogram and MS/MS spectra of PNGase A-released N-glycans from the hex-2;hex-3;aman-3 triple KO (cop1842). PA-labeled glycans were fractionated on an RP-amide column and analyzed by MALDI TOF MS/MS. Based on their elution patterns (glucose units) and MS data, predominant glycan structures detected in major HPLC peaks and key B/Y fragment ions are annotated with SNFG format and m/z values ([M+H] $^+$ ). Structural assignments are on the basis of MS/MS as well as comparisons to other studies using the same HPLC column (19, 27). MS/MS, tandem mass spectrometry; SNFG, Symbol Nomenclature for Glycans; Me, methyl; PC, phosphorylcholine.

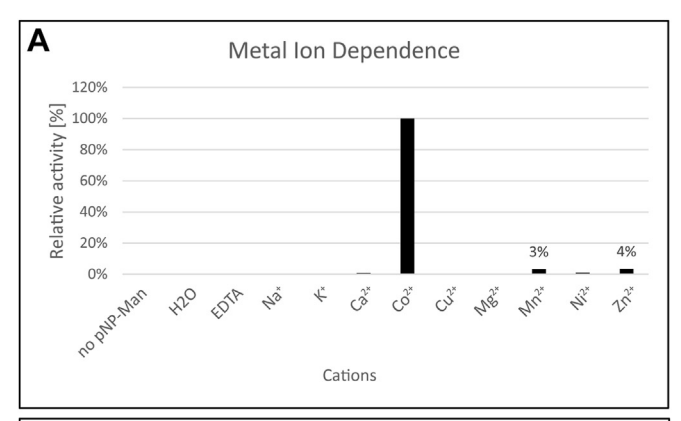
bisecting galactose or reducing terminal core  $\alpha 1,3$ -fucose found in WT N-glycomes (25, 31); in contrast, methylation of the  $\alpha 1,6$ -mannose was observed (see glycans of, *e.g.*, m/z 1206 and 1514; Fig. 4). As complex glycosylation was not blocked, but perhaps even preferred, a range of phosphorylcholine-modified N-glycans were also detected in the triple mutant (Fig. 4). Only residual amounts of glycans lacking the  $\alpha 1,6$ -mannose (late-eluting GalFuc-modified isomers of m/z 1135 and 1338) were observed.

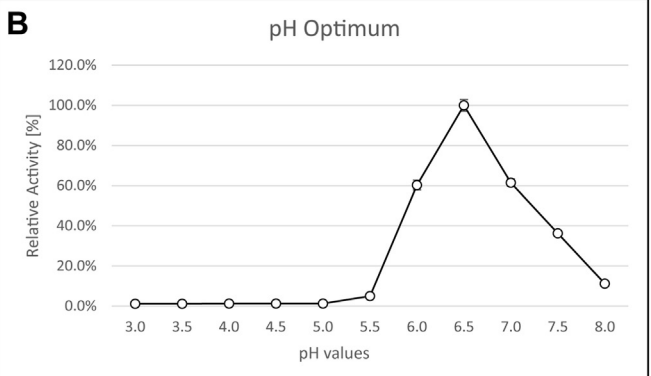
A comparison of HPLC chromatograms of N2 and *aman-3* single mutant demonstrated shifts of major peaks (Fig. S1). Tri- and tetra-fucosylated structures were observed between 10 and 14 min (5.5–7.0 g.u.). While tetra-fucosylated glycans were observed in N2 ( $\text{Hex}_{4-6}\text{HexNAc}_2\text{Fuc}_4\text{Me}_{0-1}$ ), these were completely absent in tm5400 and tri-fucosylated structures ( $\text{Hex}_{4-7}\text{HexNAc}_2\text{Fuc}_3\text{Me}_{0-1}$ ) were more pronounced in this strain (peak a, b and i to v in Fig. S1). In comparison to N2, two peaks containing primarily  $\text{Man}_3\text{GlcNAc}_2$ ,  $\text{Man}_5\text{GlcNAc}_2$ , and  $\text{Man}_3\text{GlcNAc}_2\text{Fuc}_1$  structures were decreased in tm5400 (peak c and d in Fig. S1).

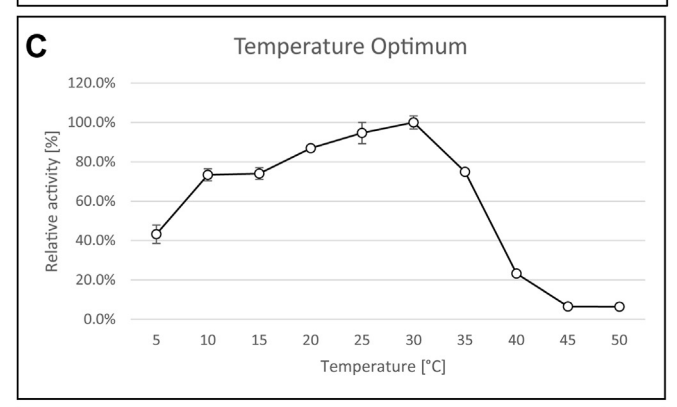
# In vitro enzymatic activity and intracellular localization of AMAN-3

The impact of deleting aman-3 on the N-glycome, especially in the hex-2;hex-3 background, directed us to more specifically examine the biochemical characteristics of the recombinant AMAN-3, which was expressed in Sf9 cells. His-tagged recombinant AMAN-3 was purified and its sequence was verified by LC-MS/MS (Table S1). The Co(II)-dependence and slightly acidic pH optimum (6.5) were confirmed (Fig. 5, A and B); AMAN-3 retained over 70% activity in a broad temperature range between 10 °C and 30 °C, whereas the activity quickly declined at temperatures above 30 °C (Fig. 5C). The pH optimum data as well as glycomic data strongly suggest that AMAN-3 is a Golgi-resident enzyme. To verify this, confocal microscopy was used to examine the distribution of GFP-fused AMAN-3 in live aman-3::egfp worms. Despite the low expression of AMAN-3, micrographs indicated that AMAN-3 signals tend to overlap with fluorescent signals of BODIPY TR ceramide, a dye used to stain Golgi apparatus (Fig. 5D).

In terms of substrate specificity, we assayed the classical Golgi AMAN-2 and novel AMAN-3 using HPLC purified N-glycans with defined structures. Only AMAN-3 removed one mannose residue from Man<sub>3</sub>GlcNAc<sub>2</sub>, Man<sub>5</sub>GlcNAc<sub>2</sub>, Man<sub>5</sub>GlcNAc<sub>2</sub>, Man<sub>5</sub>GlcNAc<sub>3</sub>, and Man<sub>5</sub>GlcNAc<sub>3</sub> as indicated by a mass shift of 162, whereas AMAN-2 only digested Man<sub>5</sub>GlcNAc<sub>3</sub>, removing two mannose residues (Figs. 6 and S2). To further investigate which substrate is favored by AMAN-3, we set reactions at room temperature with equal amount of substrate and quantified the products on HPLC. Data indicated that AMAN-3 removed solely the  $\alpha$ 1,6-mannose residue from these glycan substrates, which except for Man<sub>3</sub>GlcNAc<sub>3</sub>, resulted in shifts in HPLC retention time (Fig. 7). Full conversion was observed on Man<sub>3</sub>GlcNAc<sub>2</sub>, whereas for Man<sub>5</sub>GlcNAc<sub>2</sub>, Man<sub>3</sub>GlcNAc<sub>3</sub> and Man<sub>5</sub>GlcNAc<sub>3</sub> partial conversions (74.0%, 50.0%, and







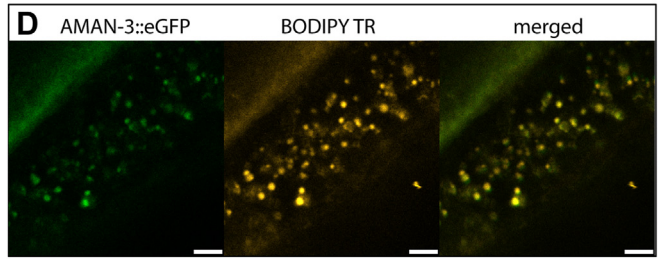


Figure 5. Enzymatic characterization of recombinant AMAN-3 and confocal micrographs of AMAN-3::eGFP worm. Analyses were performed in 96-well microtiter plates by incubating purified AMAN-3 with pNP- $\alpha$ -Man under various conditions. OD405 absorption of the reaction mixtures was measured, and relative activities were calculated by comparing obtained values with the highest value in each experiment. Impact of different metal cations on AMAN-3 was investigated, which indicated that CoCl<sub>2</sub> is a strong activator of AMAN-3 (A). The pH optimum of AMAN-3 is at 6.5 (B) and temperature optimum is at 30 °C (C). Values represent averages  $\pm$  standard errors (n=4). D, confocal images of a paralyzed adult worm demonstrate the overlapped AMAN-3::eGFP signal (green) and BODIPY signal (used to stain Golgi apparatus, shown in gold). White bars at the bottom indicate the length of 5  $\mu$ m. eGFP, enhanced green fluorescent protein.

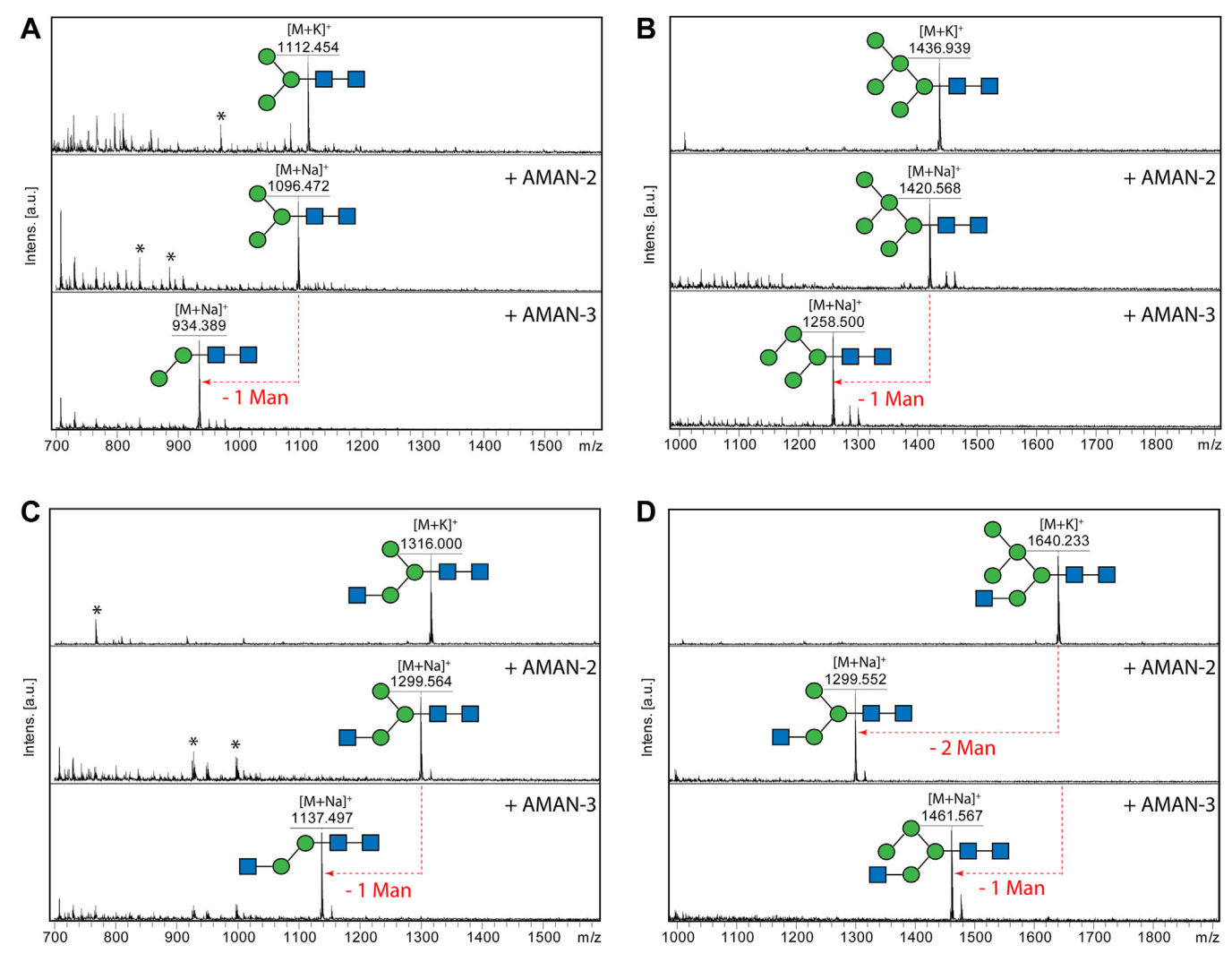


Figure 6. A comparison of substrate specificities between AMAN-2 and AMAN-3. Four RP-HPLC purified AEAB-labeled N-glycans (Man<sub>3-5</sub>GlcNAc<sub>2-3</sub>) were incubated with the recombinant mannosidases for 24 h under their optimal conditions. Reaction mixtures were measured by MALDI-TOF MS and MS/ MS. The two paucimannosidic structures Man<sub>3</sub>GlcNAc<sub>2</sub> (A, m/z 1112) and Man<sub>5</sub>GlcNAc<sub>2</sub> (B, m/z 1436) as well as a truncated complex structure Man<sub>3</sub>GlcNAc<sub>3</sub> (C, m/z 1316) are substrates of AMAN-3 but not AMAN-2, as indicated by the loss of solely the α1,6-linked mannose residue. AMAN-2 removes two mannose residues from the hybrid N-glycan Man<sub>5</sub>GlcNAc<sub>3</sub> (D, m/z 1640), whereas AMAN-3 selectively removes the terminal α1,6-linked mannose from it. Peaks marked with asterisks are nonglycan impurities. AEAB, 2-amino-N-(2-aminoethyl)benzamide; GlcNAc, N-acetylglucosamine; Man, mannose.

36.5%, respectively) were observed (Fig. 7). The partial demannosylation from Man<sub>3</sub>GlcNAc<sub>3</sub> to Man<sub>2</sub>GlcNAc<sub>3</sub> by AMAN-3 was verified by MALDI-TOF MS and MS/MS (Fig. S3).

#### Glycan remodeling using Caenorhabditis glycoenzymes

The N-glycan biosynthesis in C. elegans is a series of very complicated reactions occurring in the endoplasmic reticulum and the Golgi, resulting in a large variety of structures on properly folded glycoproteins (32). Although not yet fully understood, some of the biosynthetic pathways could be deduced from N-glycomics data obtained from WT and KO strains as well as from in vitro enzymatic data (33), whereby removal of the  $\alpha$ 1,6-mannose to result in FUT-6 substrates was considered a missing link. For the first time, we used recombinant glycosyltransferases (GLY-13, GLY-20, FUT-1, FUT-6, and FUT-8) and glycosidases (AMAN-2, AMAN-3,

and HEX-2), all recombinant forms of C. elegans enzymes, to mimic some of the biosynthetic reactions occurring in the Golgi by remodeling fluorescein containing glycoconjugates (Fig. 8).

Unlike PA-labeled and 2-amino-N-(2-aminoethyl)benzamide (AEAB)-labeled glycans, fluorescein-conjugated glycans have a tendency for in source fragmentation in MS mode; nevertheless, a portion of the intact compounds remained visible on the MS spectra. This is exemplified by analyzing the intact Man5-Fluo glycan (Fig. S4). The MS/MS spectra of [M+H-linker] tions with a mass difference of 520 Da (loss of the linker due to in-source degradation) are, however, more informative than the spectra of the intact compounds detected as [M+Na]<sup>+</sup>. Therefore, [M+H-linker]<sup>+</sup> ions were selected for structural assignment in MS/MS experiments and these m/z values are those mentioned in the following paragraphs.



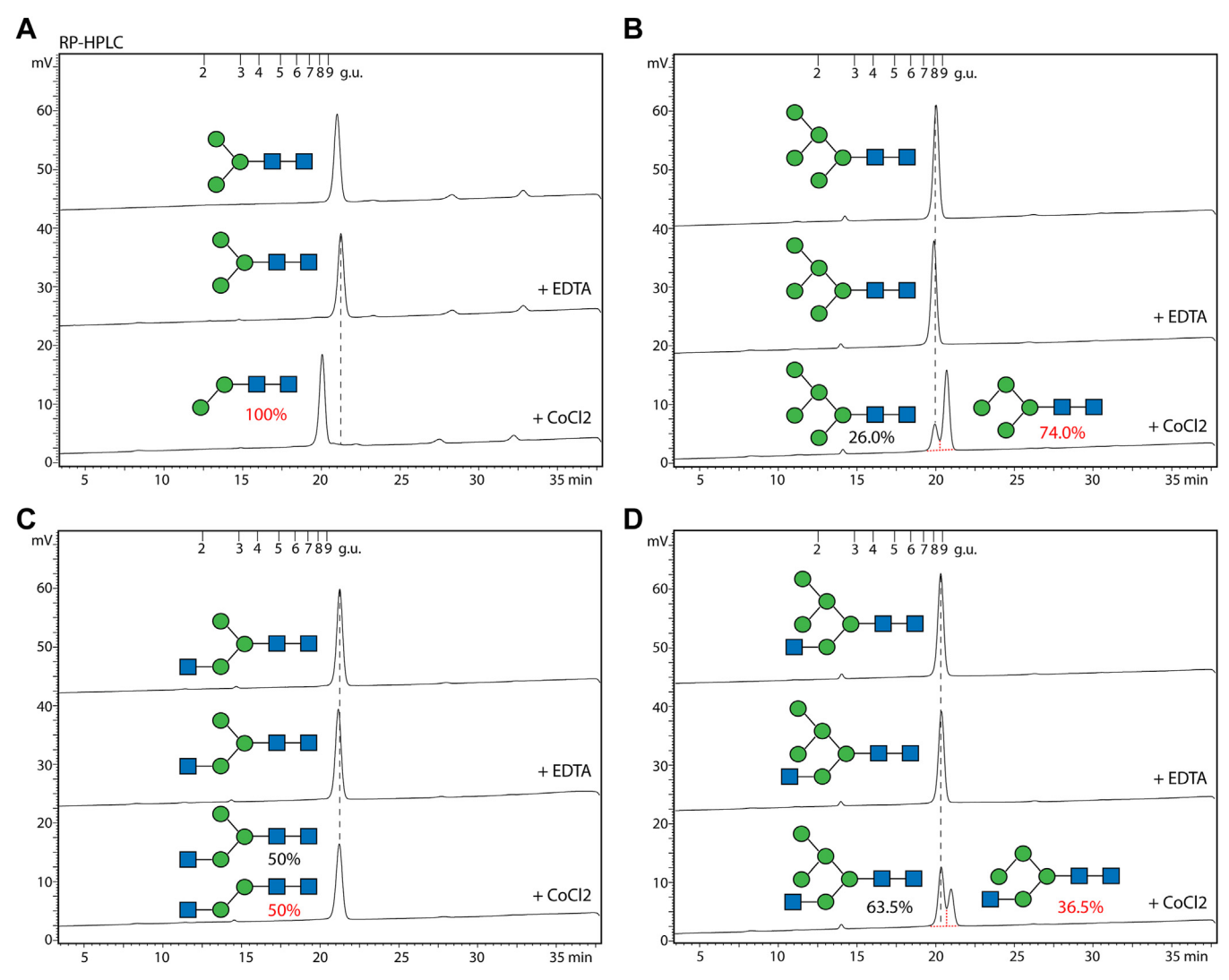


Figure 7. RP-HPLC quantification of AMAN-3 products. Equal amount of AEAB-labeled glycans (10 pmol each) were incubated with AMAN-3 in the presence of either EDTA or CoCl<sub>2</sub>. Post 16-h incubation, all samples were heat-inactivated and analyzed by HPLC on the same day. Peak areas were integrated and manually collected fractions were subject to MALDI-TOF MS analysis. Losses of one α1,6-linked mannose from Man<sub>3</sub>GlcNAc<sub>2</sub> (*A*), Man<sub>5</sub>GlcNAc<sub>2</sub> (*B*), and Man<sub>5</sub>GlcNAc<sub>3</sub> (*D*) resulted minor shifts in retention times on the chromatograms. A partial conversion of Man<sub>3</sub>GlcNAc<sub>3</sub> (*C*) to Man<sub>2</sub>GlcNAc<sub>3</sub> was confirmed by MS data (Fig. S5). AEAB, 2-amino-N-(2-aminoethyl)benzamide; GlcNAc, *N*-acetylglucosamine; Man, mannose; MS, mass spectrometry.

Firstly, an aliquot of Man5-Fluo (5 nmol) was incubated in the presence of the donor substrate UDP-GlcNAc with GLY-13, one of three known  $\beta$ 1,2-*N*-acetylglucosaminyltransferase I (GnT I) isoforms, to yield [Manα1,6(Manα1,3)Manα1,6] β1,2Manα1,3)Manβ1,4GlcNAcβ1,4GlcNAc-Fluo (Man5Gn-Fluo). Full conversion was observed after overnight incubation as judged by the ion of m/z 1420, increased by 203 from m/z 1217 (Fig. 8A); in addition, a portion of the GnT I product was fully fucosylated by a \$\alpha 1,6-fucosyltransferase (FUT-8), which resulted in the formation of a compound with m/z 1566 (corresponding to Fig. 8B). The core fucosylation has been confirmed by the presence of a daughter ion HexNAc<sub>2</sub>Fuc<sub>1</sub> of m/z 553.5, a diagnostic ion used for other compounds carrying 6-linked core fucose residue. Under the same conditions, a small aliquot of Man5-Fluo was fully fucosylated by FUT-1 to [Manα1,6(Manα1,3)Manα1,6] (Manα1,3)Manβ1,4GlcNAcβ1,4

(Fucα1,3)GlcNAc-Fluo and in this case its daughter ion Hex-NAc<sub>1</sub>Fuc<sub>1</sub> (m/z 350.5, Fig. 8C) was more pronounced in the MS/MS spectrum. However, C elegans FUT-8 cannot modify Man5-Fluo with a 6-linked core fucose *in vitro*, even though more enzyme was added and longer incubation was carried out, suggesting that this enzyme strictly requires the presence of GlcNAc on the lower arm of the reducing end. Interestingly, the observation of N-glycans with core  $\alpha$ 1,6-fucose (minor portion) in a triple GlcNAc-TI KO indicated *in vivo* activity of FUT-8 on Man5-carrying glycoproteins (12). This enzymatic characteristic is identical to the human homologous enzyme FUT-8 published recently (34).

Following modification by GLY-13, Man5Gn-Fluo was processed by a Golgi  $\alpha$ -mannosidase AMAN-2 without previous purification; a new compound with m/z 1096 was observed after 2-h incubation, indicative of a full conversion to Man- $\alpha$ 1,6(GlcNAc $\beta$ 1,2Man $\alpha$ 1,3)Man $\beta$ 1,4Glc-NAc $\beta$ 1,4GlcNAc-Fluo

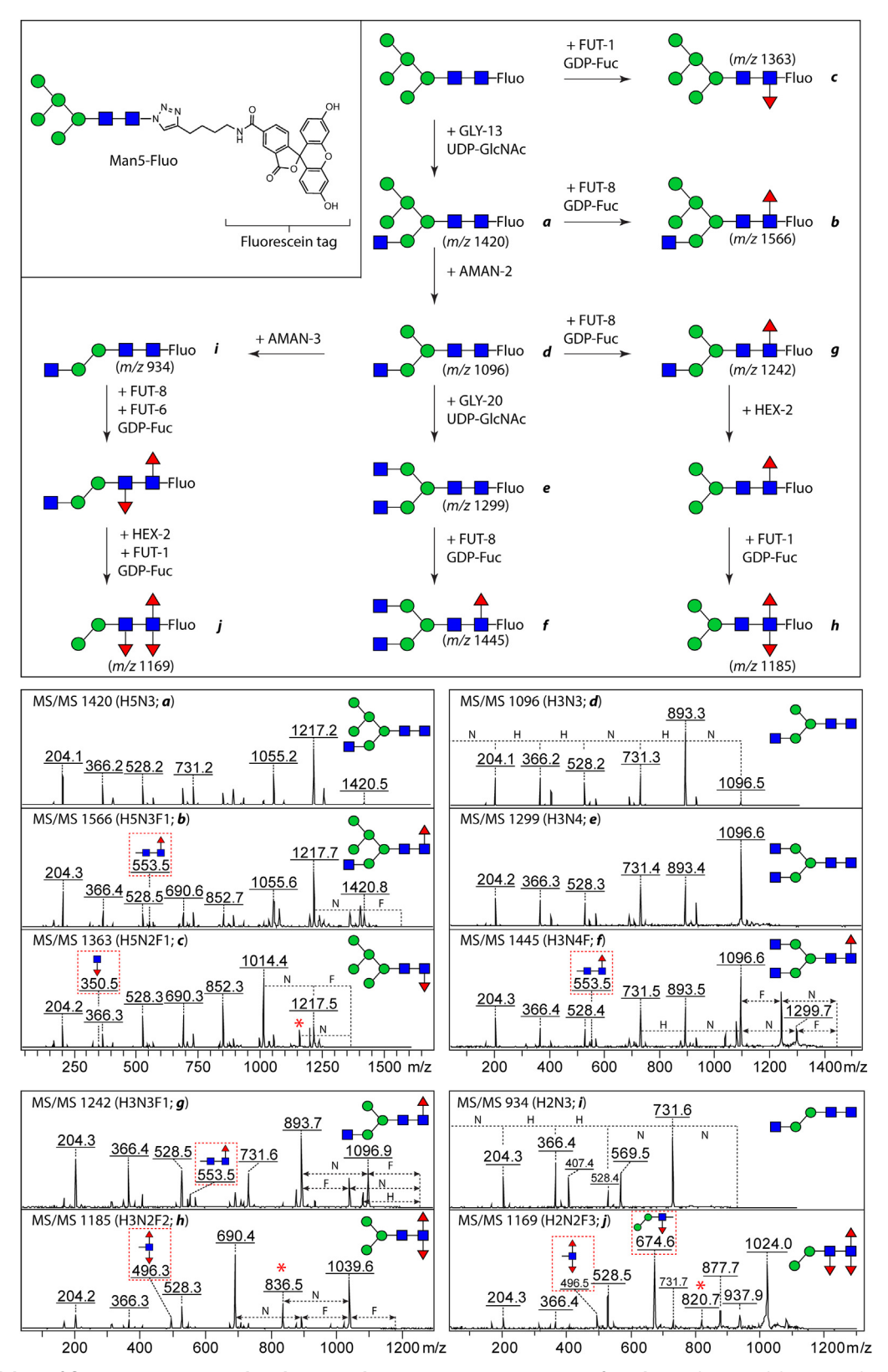


Figure 8. Remodeling of fluorescein-conjugated N-glycans and MALDI-TOF MS/MS spectra of products. The remodeling started with a Man<sub>5</sub>GlcNAc<sub>2</sub> structure; 5 Caenorhabditis elegans glycosyltransferases as well as three glycosidases, recombinantly expressed in Pichia pastoris, were sequentially used to modify their substrates; afterward, aliquots of the reaction mixtures were analyzed by mass spectrometry. A range of hybrid, complex biantennary, and fucosylated paucimannosidic N-glycan structures were successfully synthesized. Structures of enzymatic products (a to j, left panel) were confirmed based on the fragmentation patterns of their parent ions ([M+H-linker]+), as well as the knowledge of the substrate specificities of the employed enzymes. Key fragments indicating where fucose is attached were highlighted in dashed boxes in red; whereas fragment ions, indicative of the "re-arrangement" of fucose residues, were marked with red asterisks (e.g., m/z 836.5).



(also known as MGn; Fig. 8D). Subsequently, HPLC purified MGn-Fluo was split for further remodeling into two types of N-glycans: biantennary glycans and fucosylated glycans. The former were achieved by sequential incubation with GLY-20 and FUT-8; the two products were verified by MS/MS (m/z 1299 and 1455, Fig. 8, E and F). A difucosylated glycan was created by serial incubation of MGn-Fluo first with FUT-8 to introduce 6-linked fucose and then with a mixture of HEX-2 and FUT-1 to introduce a 3-linked fucose (Fig. 8, G and *H*). The final product carries Man $\alpha$ 1,6(Man $\alpha$ 1,3)Man $\beta$ 1, 4Glc-NAcβ1,4(Fucα1,6)(Fucα1,3)GlcNAc-Fluo (also called MMF<sup>3</sup>F<sup>6</sup>), which is a typical difucosylated N-glycan occurring in both nematodes and insects (7, 35); this structure was concluded due to a range of daughter ions including m/z496.3 Y-ion and its corresponding B-ion of m/z 690.2, suggesting a difucosylation on the inner most nonreducing GlcNAc residue.

In addition, by removing the "upper arm" from MGn-Fluo with AMAN-3, a FUT-6 acceptable substrate was formed (Fig. 8*I*). After sequential modification with core FUTs and HEX-2, removing the nonreducing GlcNAc residue, a trifucosylated glycan Man $\alpha$ 1,3Man $\beta$ 1,4(Fuc $\alpha$ 1,3)GlcNAc $\beta$ 1,4(Fuc $\alpha$ 1,6) (Fuc $\alpha$ 1,3)GlcNAc-Fluo was achieved as judged by the presence of fragments at m/z 496.5 and 674.6 (Fig. 8*J*).

These results provided additional enzymatic data to support the sequential modifications of N-glycans by Golgi residentglycoenzymes toward the formation of hybrid-, biantennary-, and fucosylated paucimannosidic N-glycans.

# Loss of glycosylation enzymes delays development, reduces animal size, and impairs food-dependent behaviors

The phenotypic characterization of C. elegans glycomutants used in this study offer an opportunity to further define the biological role of N-glycan modifying enzymes in vivo. All homozygous strains were viable under laboratory conditions and naked eye observation with a regular stereo microscope did not show obvious phenotypes. We thus turned to quantitative assessments of worm growth speed, size, posture, and locomotion. First, we measured the developmental speed by comparing the time from hatching to first egg-laying in WT (N2), bre-1, aman-3, as well as hex-2;hex-3 double mutants, and hex-2;hex-3;aman-3 triple mutants (Fig. 9, A and B). We found that bre-1, aman-3, and hex-2;hex-3 developed significantly slower than WT (Fig. 9A). Interestingly, the hex-2;hex-3;aman-3 triple mutant growth was similar to that of N2 and significantly faster than that of either aman-3 or hex-2;hex-3, suggesting that these mutations genetically interact to modulate developmental speed.

Second, we quantified the size of adult animals (Fig. 9, *B–E*). Whereas the size of *hex-2;hex-3* double mutants was similar to that of WT, it was significantly reduced in *bre-1*, *aman-3*, and *hex-2;hex-3;aman-3* triple mutants. Both animal length and midbody width were reduced in *bre-1* and *aman-3*, whereas only length was reduced in *hex-2;hex-3;aman-3* triple mutants (Fig. 9, *D* and *E*).

Third, we used high-content computer-assisted behavioral analysis tools to reveal postural and locomotion differences

across strains in crawling animals under fed and starved conditions. On food, WT animals are in a dwelling state (36, 37), characterized by low locomotion speed, frequent pausing, and foraging head movement (side-to-side nose swipes). All four mutant strains displayed altered dwelling behavior, with upregulated foraging movements and downregulated pausing frequency (Fig. 10, A-C). As in previous studies (37), fooddeprivation caused WT worms to shift to a food-search behavior characterized by increased speed (Fig. 10D) and more frequent reorientation events (called omega turns, Fig. 10E), hence producing specific dispersal trajectories (Fig. 11A), favoring longer-range exploration (Fig. 11B). This behavioral state is also associated with a distinct posture, including increased midbody and tail bending (Fig. 10, F and G). We found that, upon food deprivation, the bre-1 mutants and aman-3 mutants displayed reduced speed, omega turn frequency, midbody, and tail bending as compared to WT (Fig. 10, D-G). Examples of typical postures with reduced curvature are presented in Fig. S5. In contrast, hex-2;hex-3 double mutants had an opposite phenotype with increased speed and omega turn frequency (Fig. 10, D and E). The triple hex-2;hex-3;aman-3 mutant displayed even further increase in speed and omega-turn frequency, with values significantly increased in comparison to all the other genotypes. These specific behavioral differences across genotypes were associated with different trajectories and dispersal efficacy, that is likely relevant for food-search behavior (Fig. 11).

Collectively, our phenotypic data in glyco-mutants highlights a role for *aman-3*, *hex-2/3* and *bre-1* in controlling worm developmental speed, animal size, dwelling behavior on food and food-search behavior in response to food-deprivation. Furthermore, the various phenotype-specific genetic interaction types between *aman-3* and *hex-2;hex-3* mutations suggest that the complex, nonadditive impact that the losses of AMAN-3 and the two hexosaminidases have on N-glycan structures translates into pleiotropic phenotypic impact.

#### Discussion

Probably all multicellular eukaryotes have multiple members of the so-called GH38 α-mannosidase family. At least one is lysosomal or vacuolar and involved in glycoconjugate degradation, whereas one or more have roles in N-glycan remodeling in the Golgi apparatus (38). In a previous study, the C. elegans AMAN-3 was identified as a homolog of the Golgi α-mannosidase II (AMAN-2) and the nonpurified recombinant enzyme showed to react with pNP-α-mannoside, an artificial substrate (23). Here, we confirm and expand on these previous observations to substantiate the notion that AMAN-3 is a Golgi-resident α1,6-mannosidase that uses Nglycans as substrates, representing a sought-after missing link in the N-glycan biosynthetic pathway of C. elegans and a number of related nematode species, and filling an important gap in our understanding of the complex of enzymatic reactions.

AMAN-3 fits the characteristics of typical Golgi-resident mannosidases, which possess N-terminal transmembrane



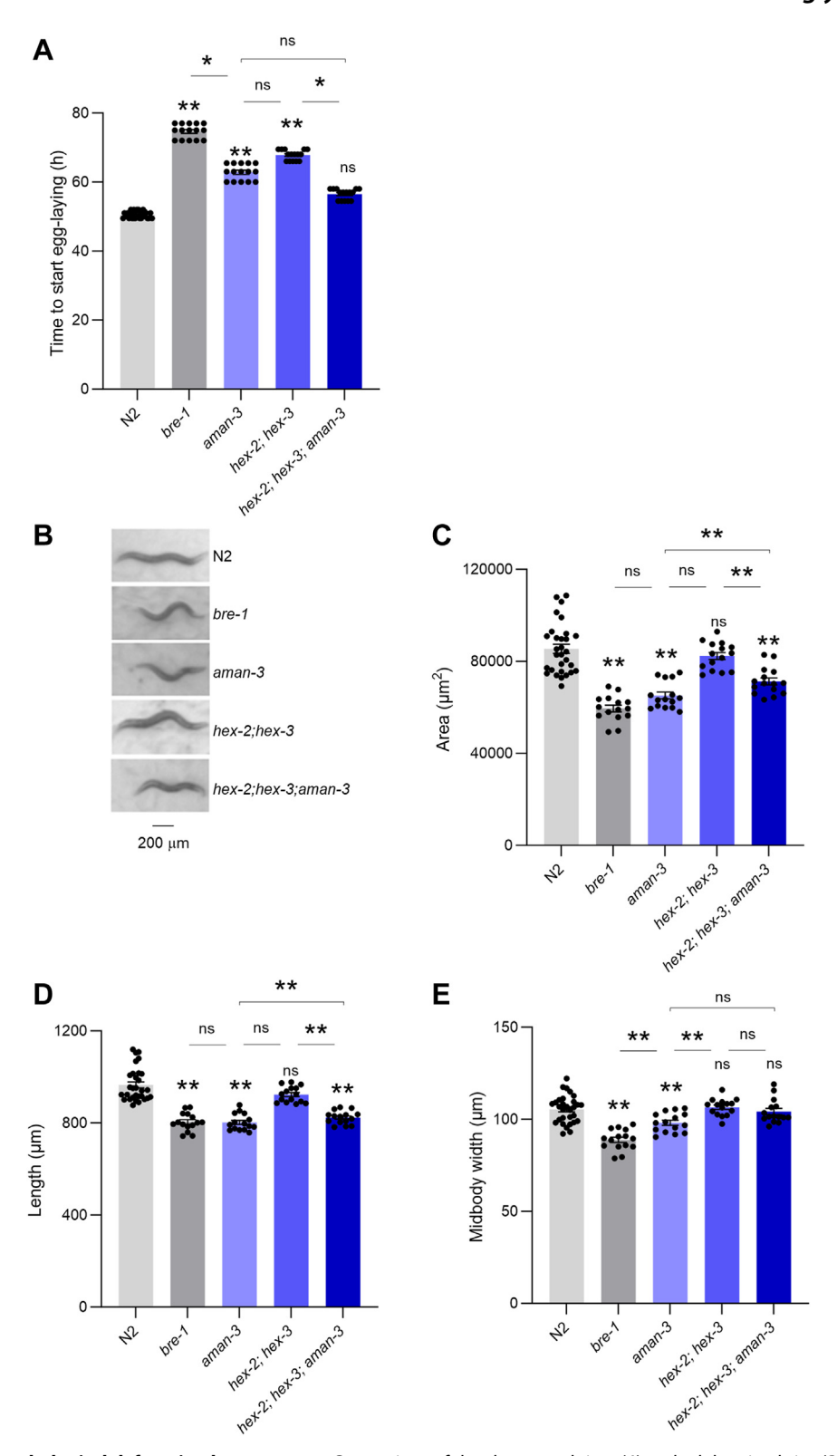


**Figure 9. Growth and morphological defects in glyco-mutants.** Comparison of developmental time (A) and adult animal size (B–E) between WT (N2) and indicated glyco-mutants grown at 25 °C. Average (bars)  $\pm$  s.e.m. (error bars) of n = 15 assays per genotype, each assay scoring at least 20 animals (A, C–E). Representative picture of adult worms illustrating size differences (B). \*\*p < 0.01; \*p < 0.05, ns, not significant by Dunn (A) or Bonferroni (C–E) post hoc tests. Signs just above the glyco-mutant bars indicate significance levels *versus* N2.

domains, are active at a slightly acidic pH and require metal ions as cofactors (23). Our GFP-fusion confocal data in this study are also in line with a Golgi localization of AMAN-3.

Interestingly, AMAN-3 activity depends on the presence of Co(II) as divalent metal ion. This feature is very similar to a *Spodoptera frugiperda* Golgi  $\alpha$ -mannosidase, the SfMANIII, as



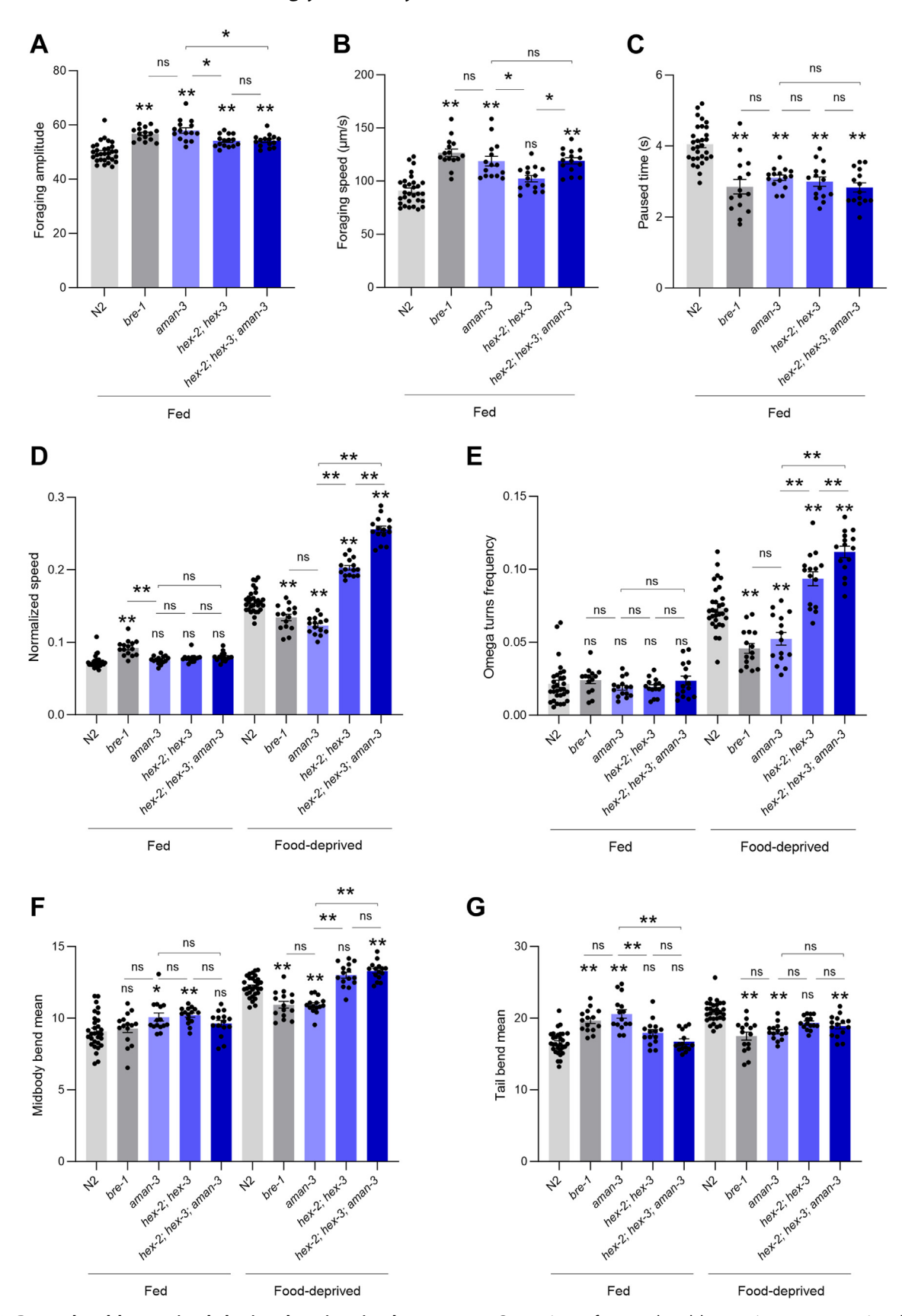


Figure 10. Postural and locomotion behavior alterations in glyco-mutants. Comparison of postural and locomotion parameters in adult animals between WT (N2) and indicated glyco-mutants grown at 25 °C and assessed on food (Fed, A–G) or assessed off-food 3 h after food deprivation (Food-deprived, D–G). Average (bars)  $\pm$  s.e.m. (error bars) of n = 15 assays per genotype, each assay scoring at least 20 animals. \*\*p < 0.01; \*p < 0.05, ns, not significant by Bonferroni (A-G) post hoc tests. Signs just above the glyco-mutant bars indicate significance levels versus N2.

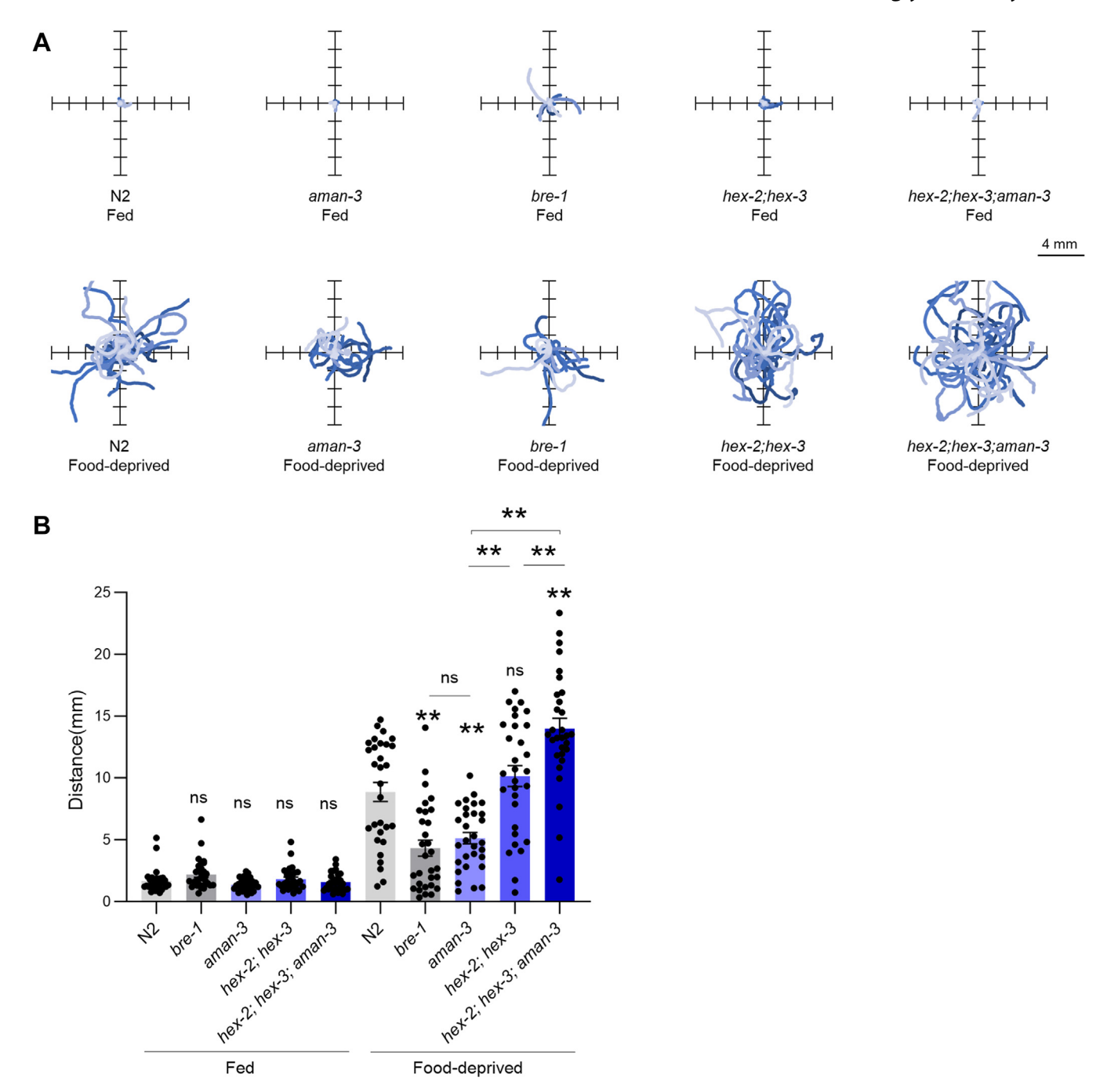


Figure 11. Alteration of food-search trajectories in glyco-mutants. One-minute worm trajectories of well-fed worms on food (A, top panels) and 3 h food-deprived worms off-food (A, bottom panels). Thirty trajectories per condition plotted from a single starting (0,0) coordinate and illustrating the worm dispersal. Average  $\pm$  s.e.m. and individual data points for the covered distance (B, corresponding to the path length). n=30 animals. \*p<0.05 and \*\*p<0.05 and \*\*p0.01 by Bonferroni post hoc tests. Signs just above the glyco-mutant bars indicate significance levels versus N2.

well as the Drosophila Man-IIb (Table 1). Both insect and nematode enzymes can be inhibited by swainsonine, a common GH38 α-mannosidase inhibitor (21, 22). Other Co (II)-dependent mannosidases include cytosolic or lysosomal enzymes with roles in degradation, such as mammalian MAN2C1 and MAN2B2 (39, 40).

In this study, we used reverse genetics and comparative glycomics to obtain a very detailed view of the impact of aman-3 loss, and combined these approaches with a

comprehensive in vitro reconstitution system of glycan remodeling able to reveal AMAN-3 action in the context of a complex substrate pool. Our glycomics data provided direct evidence that the aman-3 gene is essential to the biosynthesis of tetra-fucosylated N-glycans occurring in the N2 WT worms. Knocking out aman-3 in hex-2;hex-3 double mutant resulted in an even more dramatic shift in the N-glycome, as judged by the absence of fucose modification on the distal GlcNAc residue. One signature glycan structure in hex-2;hex-3 with a



Table 1 A comparison of insect and nematode Golgi α-mannosidase III

Enzymes	SfManIII	Dm ManIIb	Ce AMAN-3
Characteristics	GnT I-independent	GnT I-independent	GnT I-independent
Optimal pH	6.5	5.8	6.5
Optimal temperature	n.a.	37 °C	30 °C; >70% activity at 10-30 °C
Inhibitor	Swainsonine	Swainsonine	Swainsonine
Substrates	Man <sub>6-9</sub> GlcNAc <sub>2</sub>	Man <sub>8-9</sub> GlcNAc <sub>2</sub>	Man <sub>3</sub> GlcNAc <sub>2</sub>
	Man <sub>5</sub> GlcNAc <sub>2</sub>	Man <sub>5</sub> GlcNAc <sub>2</sub>	Man <sub>5</sub> GlcNAc <sub>2</sub>
			Man <sub>3</sub> GlcNAc <sub>3</sub>
			Man <sub>5</sub> GlcNAc <sub>3</sub>
Cobalt activation	Yes	Yes	Yes
Specificity	α1,2-linked mannose	α1,2-linked mannose	α1,6-linked mannose
	α1,3/6-linked mannose	a1,3/6-linked mannose	
Reference	Kawar et al. (21)	Nemčovičová et al. (22)	Paschinger et al. (23) and data in this study

composition of Man<sub>2</sub>GlcNAc<sub>3</sub>Fuc<sub>2</sub>Gal<sub>2</sub> is completely abolished (Fig. 12). Collectively, our data indicated that AMAN-3 plays a key role in removing a "block" to modification by FUT-6 of the distal (second) core GlcNAc residue. Thus, it can be surmised that orthologues of AMAN-3 work in concert with orthologues of FUT-6 in species such as H. contortus, O. dentatum, and A. suum, but that these are absent from species such as D. immitis or T. suis which lack trifucosylated core chitobiose motifs (9, 20, 41). The biological role of these structures in the context of parasite-host interactions remains unclear. However, it is possible that mammalian hosts recognize these structures of parasites, as they significantly differ from mammalian glycans. Indeed, the question as to how the natural processing of parasite antigens affects their immunogenicity as well as their ability to act as protective epitopes is still open. Studies on H. contortus H11 antigens have indicated that recombinant forms do not induce protective immunity, even if expressed in C. elegans (42); however, the ability to better reproduce natural H. contortus glycosylation in

recombinant expression systems by using AMAN-3 and FUT-6 may bring us closer to understanding the interplay between nematode glycosylation and host immune systems.

Beyond its likely relevance for parasite-host interaction, our study provides direct insight on the more general biological importance of AMAN-3, BRE-1, and HEX-2/3 enzymes in C. elegans, including their roles in growth and behavior modulation. Interestingly, our data show that the different mutations produce sometime similar and sometimes opposite impact on the different phenotypic parameters. For instance, bre-1 and hex-2/-3 mutations both reduce growth speed, but their respective impact on animal speed and omega turn during food search was opposite. Likewise, the epistatic analysis between aman-3 and hex-2;hex-3 showed different synthetic effects, with positive epistasis effects for food-search behavior parameters, but a negative epistasis effect for development speed. These complex phenotypic patterns are not very surprising in the light of the complex glycome alterations that these mutations produce, which are not "simply additive".

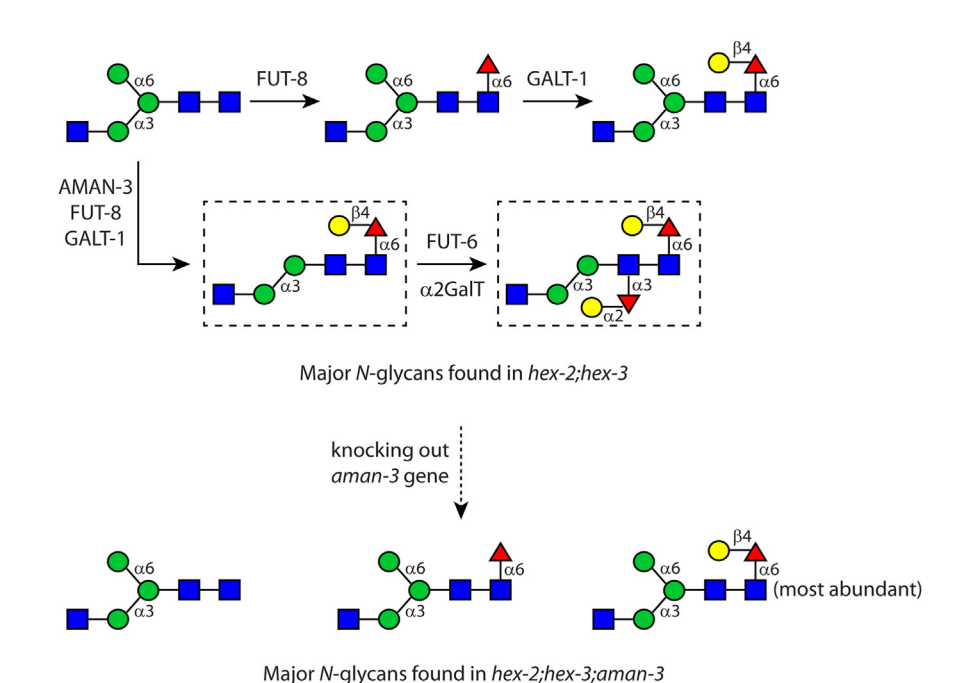


Figure 12. A summary of major N-glycan structures found in the double (hex-2;hex-3) and in the triple (hex-2;hex-3;aman-3) mutants. Enzymes that participate relevant biosynthetic pathways are annotated. Glycans without the "upper arm" (shown in dashed boxes), abundant in hex-2;hex-3, are abolished after knocking out the aman-3 gene.

Indeed, each mutant produces a unique pattern of N-glycans, missing some WT structures and harboring some abnormal structures (Figs. 3 and 4). Behavioral differences observed in worm glyco-mutants demonstrated a close connection between protein glycosylation and developmental defects as exemplified by studies on *aman-2* and *cogc* mutants (43, 44), which is also well-known in human congenital disorders of glycosylation (45). Our approach combining glycome data with high-content phenotypic characterization paves the road for future studies with additional *C. elegans* glyco-mutants in order to get a more comprehensive and systematic understanding of the relationships between glycome changes and their phenotypic impact in this powerful genetic model.

#### **Experimental procedures**

### Preparation and cultivation of C. elegans strains

The N2 WT C. elegans and HY496 mutant (bre-1 deficiency) were obtained from the Caenorhabditis Genetics Center, University of Minnesota, MN and an aman-3(tm5400) single mutant, carrying a 401 bp deletion and 2 bp insertion in the aman-3 gene, was obtained from the National Bioresource Project for the Experimental Animal Nematode C. elegans, Tokyo Women's Medical University, Japan. A hex-2;hex-3 double mutant (16) was previously prepared by crossing the single hex-2(tm2530) mutant and hex-3(tm2725) mutant, which were obtained through the National Bioresource Project; this double mutant was used to prepare a hex-2;hex-3;aman-3 triple mutant (cop1842) using the CRISPR/Cas9 approach by Knudra Transgenics (NemaMetrix). Using two aman-3-targeting sgRNAs to guide Cas9, a 5145-bp fragment was deleted in the genome of the hex-2;hex-3 mutant and replaced with a 18-bp insertion containing a 3-frame stop sequence (5'-TAAATAAATAAACTCGAG-3'). Screening was carried out by genotyping PCR using primer pairs A (5'-AGCCTCAATTTCGTCTACACCAC-3' and 5'-GGG CAAATCGGAGTCATCTGAA-3', 652 bp as the WT) and B (5'-AGCCTCAATTTCGTCTACACCAC-3' and 5'-CCTGTT TTGCACCCAGTTTGATG-3', 724 bp as aman-3 KO, Fig. S6) and the deletion of aman-3 gene was confirmed by DNA sequencing. Moreover, an enhanced green fluorescent protein (eGFP)-encoding DNA fragment was fused to the aman-3 gene of N2 worms using CRISPR/Cas9 technology. This knock-in strain (aman-3::egfp, strain name PHX5021; allele syb5021) was custom-made by SunyBiotech.

All worm strains were cultured under standard conditions at 20  $^{\circ}$ C. For a large-scale preparation, worms were grown in Scomplete medium supplied with *Escherichia coli* OP50 in shake flasks and were purified by sucrose density centrifugation; after intensive washing in saline solution, worms were stored at -80  $^{\circ}$ C prior to analysis.

#### Mannosidase activity assays using worm lysate

N2, *aman-3*, and *hex-2;hex-3* worms were harvested from nematode growth medium agar plates and repeatedly washed in saline solution (0.9% NaCl) to remove OP50. Worms were transformed in a tissue grinder and

homogenized in 300  $\mu$ l of lysis buffer containing 20 mM Mes buffer, pH 6.9, 0.5% Triton X-100, and 0.01% protease inhibitor cocktail (Sigma-Aldrich); post centrifugation to remove cell debris (14,000g for 4 min at 4 °C) clear supernatants of the worm lysates were kept for enzymatic assays. Reaction mixtures were prepared by mixing 1  $\mu$ l of PA-MM substrate (2D-HPLC purified) and 0.8  $\mu$ l of worm supernatant with 25 mM ammonium acetate buffer (pH 6.5) supplied with or without 6 mM cobalt (II) chloride (CoCl<sub>2</sub>) or 0.6  $\mu$ M Swainsonine (Sigma-Aldrich). Reactions were incubated at room temperature prior to HPLC analysis.

#### Confocal microscopy

Worms at mixed developmental stages were harvested and incubated in M9 buffer supplied with 5  $\mu$ M BODIPY TR Ceramide complexed to bovine serum albumin (Invitrogen) at room temperature (1 h). Prior to immobilization on poly-Llysine–coated glass slides, worms were thoroughly washed in M9 and paralyzed in 20 mM levamisole hydrochloride (Sigma-Aldrich). Images were recorded using a Leica TCS SP5 laser scanning confocal microscope (Wetzlar) as described previously (27).

#### Molecular cloning

Reagents and kits used for molecular cloning are mostly purchased from the New England Biolabs unless specified. DNA oligonucleotides were ordered from Sigma-Aldrich. The C. elegans aman-2 coding sequence was subcloned from a pPICZαC construct (23) to a reengineered pPICαHisFLAG vector (15) using the Gibson Assembly (GA) approach. GA primers (5'-CGACGATGACAAGCTGCAGGCATCGATGAAAGATG TTTGTGG-3' and 5'-GCTGGCGGCCGCCCGCGGTTAAA ATGATACAAGAATACTG-3') were used to amplify a truncated aman-2 gene (encoding aa 126-1145) by two-step PCR using a Q5 HIFI DNA polymerase; DNA fragment was ligated to an empty pPICαHisFLAG vector using NEBuilder HiFi DNA Assembly Cloning Kit and the reaction mixture was transformed to NEB5\alpha competent cells. Followed by PCR screening, constructs of positive clones were DNA sequenced (LGC genomics). The aman-2 construct was linearized by Pme I, purified and transformed by electroporation to the GS115 strain of Pichia pastoris for protein expression. (Note that despite previous success with an untagged AMAN-3 (23), an N terminally tagged form was not expressed; thus, insect cellbased expression was employed as described below.)

To express AMAN-3 in insect cells, the truncated *aman-3* gene (encoding aa 35–1046) was PCR amplified (5'-GCAGC-CATCAAAGATTAGGACAGCA-3' and 5'-CGTCGACG-TAGGTCATCGATAAAGAATCAA-3') and ligated in-frame to an engineered pACEBac1 vector (Fig. S7), which contains DNA fragments encoding a melittin signal sequence (MKFLVNVALVFMVVYISYIYA), a His-FLAG tag (HHH HHHDYKDDDDK) and a thrombin cleavage site (LVPRGS) on the N terminus of AMAN-3. This construct is incorporated into the baculovirus genome following the instruction provided with the MultiBac cloning kit (Geneva Biotech).



#### Recombinant protein expression and purification

Recombinant forms of *C. elegans* AMAN-2 (with or without a His-tag), AMAN-3 (nontagged) (23), GLY-13 (nontagged), GLY-20 (nontagged) as well as His-tagged HEX-2 (46), FUT-1, FUT-6, and FUT-8 (12) were expressed in *P. pastoris* for 72 to 96 h at 16 °C following the manufacturer's manual. Methanol was added to the culture daily to maintain an induction concentration at 1%. Harvested culture supernatants were concentrated and buffer-exchanged by ultrafiltration using 30 kDa molecular weight cutoff centrifugal devices (Sartorius). Hand-packed nickel affinity columns (Qiagen) were used to obtain purified recombinant proteins that carry an N-terminal poly-histidine tag (AMAN-2, HEX-2, and FUTs).

His-tagged AMAN-3 was expressed in Sf9 insect cells. Briefly, cells were maintained in HyClone SFM4Insect medium (GE HealthCare) supplied with 3% of fetal bovine serum (Gibco) at 27 °C. Post transfection of Sf9 cells with a Bacmid DNA (2  $\mu$ g) using 10  $\mu$ l of FuGene (Promega), recombinant baculoviruses carrying *aman-3* gene were harvested (V<sub>0</sub>) and used to infect Sf9 cells in a 68 ml suspension culture (80 rpm, 27 °C). 3 days post infection, the recombinant AMAN-3 was purified from the cell culture supernatant by His-tag purification. The protein sequence was verified by LC-MS/MS at the MS core facility of the University of Veterinary Medicine Vienna.

#### Mannosidase activity assays using recombinant enzymes

To assess the biochemical property of AMAN-3, including metal ion dependency, temperature and pH optima, a colorimetric assay using p-nitrophenyl- $\alpha$ -mannopyranoside as a substrate (pNP-Man, dissolved in dimethyl sulfoxide) and Co(II) was employed as previously described (23). Briefly, His-Tag-purified AMAN-3 was incubated with 5 mM pNP-Man in quadruplicate in a 96-well plate under various conditions using McIlvaine buffers. Post terminating the reactions with 250  $\mu$ l of 0.4 M glycine-NaOH, pH 10.4, absorbance at 405 nm ( $A_{405}$ ) were measured using a Tecan Infinite M200 micro-plate reader.

To generate N-glycan substrates for testing recombinant mannosidases, a Man<sub>8</sub>GlcNAc<sub>2</sub> structure conjugated with *AEAB* (purchased from NatGlycan LLC) was remodeled. Subsequently, 10 nmol of this compound was first digested with α1,2-mannosidase (New England Biolabs; yielding Man<sub>5</sub>GlcNAc<sub>2</sub>) and then processed by GLY-13 in the presence of donor substrate UDP-GlcNAc and Mn (II) (yielding Man<sub>5</sub>GlcNAc<sub>3</sub>). Man<sub>3</sub>GlcNAc<sub>3</sub> and Man<sub>3</sub>GlcNAc<sub>2</sub> structure were prepared by digesting Man<sub>5</sub>GlcNAc<sub>3</sub> with AMAN-2 alone or in combination with HEX-2. All resulted compounds were HPLC purified and quantified based on the integrated areas of corresponding eluent peaks.

#### Release of N-glycans and PA-labeling

*C. elegans* strains at mixed-stages (4–6 g in wet weight) were boiled in water to denature endogenous proteases and glycosidases; worms were homogenized in a tissue grinder prior to a 2-h proteolysis at 70  $^{\circ}$ C in a round-bottom glass flask using

thermolysin (Promega, 1 mg per 1 g wet-weight worm) in 50 mM ammonium bicarbonate buffer (pH 8.5) supplied with 0.5 mM CaCl<sub>2</sub> (25). Post centrifugation to remove insoluble cell debrides, glycopeptides were enriched by cation exchange chromatography (Dowex 50W × 8; elution with 0.5 M ammonium acetate, pH 6.0) and desalted by gel filtration (Sephadex G25, 0.5% acetic acid as solvent). N-linked glycan was released using a recombinant Oryza sativa PNGase A (New England Biolabs) in 50 mM ammonium acetate buffer (pH 5.0) overnight at 37 °C. Native glycans were separated from residual peptides by cation exchange chromatography (Dowex 50W  $\times$  8); glycans collected in the filtrate fraction (as no longer bund to the column) were further purified using hand-packed C18 cartridges and nPGC cartridges prior to analysis. Native glycans were labeled with 2-aminopyridine (PA) to induce a fluorescent tag at the reducing ends, and the excess reagent was removed by gel filtration (Sephadex G15, 0.5% acetic acid as solvent) as previously described (25).

#### Glycan remodeling

In total, eight active enzymes (AMAN-2, AMAN-3, GLY-13, GLY-20, HEX-2, FUT-1, FUT-6, and FUT-8) were used for the remodeling experiments. All recombinant enzymes were expressed in-house as described above. Except for His-tagged enzymes that were purified, crude enzymes post concentration and buffered-exchange against a storage buffer (25 mM Tris–HLC, 150 mM NaCl, pH 7.0) were used. A fluorescein-conjugated  ${\rm Man}_5{\rm GlcNAc}_2$  structure (Man5-Fluo) was chemically synthesized and verified by NMR (detailed in Supporting information).

In brief, 5 nmol of Man5-Fluo was used as the initial acceptor substrate, sequentially modified by glycosyltransferases and glycosidases according to the experimental design (Fig. 8). For assays using glycosyltransferases, mixtures containing 80 mM MES buffer (pH 6.5), 20 mM MnCl<sub>2</sub>, substrate, 2 mM nucleotide sugar and relevant enzyme were prepared, whereas for assays using glycosidases, mixtures containing 160 mM Mes buffer, substrate and relevant enzyme were prepared. Incubation was carried out overnight at 37 °C to ensure the full conversion, except for AMAN-2 which was incubated for 2 h to reduce a by-product. Reaction mixtures were directly analyzed by MALDI TOF MS, and a few reaction products were HPLC purified prior to MS analyses to obtain improved MS and MS/MS data.

#### **HPLC** methods

A Shimadzu Nexera UPLC system equipped with a RF 20AXS fluorescence detector was used to analyzed and fractionate different glycoconjugates. For N-glycomics studies, 2-aminopyridine (PA)-labeled worm glycans were fractionated over an Ascentis RP-amide column (2.7  $\mu$ m, 15 cm  $\times$  4.6 mm attached to a 5 cm guard column; Sigma-Aldrich) on HPLC. A gradient of 30% (v/v) methanol (buffer B) in 0.1 M ammonium acetate, pH 4.0 (buffer A) was applied at a flow rate of 0.8 ml/min as follows: 1% buffer B per minute over 35 min (excitation/emission: 320 nm/400 nm) (17). In addition, separation of

PA-glycans was also achieved using a Hypersil ODS column (Agilent Technologies) with the same buffers and detector settings, but a flow rate of 1.5 ml/min.

A HyperClone reversed phase column (5µ ODS C18, 250 × 4 mm; Phenomenex) was used for the separation and quantification of AEAB-labeled N-glycans and the purification of fluorescein-conjugated glycans. AEAB-glycans: 0.1 M ammonium acetate, pH 4.0 as buffer A and 30% (v/v) methanol as buffer B, and an optimized gradient as follows: 0 to 10 min, 0 to 20% B; 10 to 35 min, 20 to 50% B; 35 to 35.5 min, 50% B; 35.5 to 36 min, 0% B; 36 to 40 min, back to starting conditions. The flow rate was set at 1.5 ml/min with a maximal pressure at 375 bars and the fluorescence detector setting was Ex 330 nm and Em 420 nm. Fluoresceinglycans using 0.1% formic acid as buffer A and a mixture of 99.9% acetonitrile and 0.1% formic acid as buffer B; detector setting was Ex 490 nm and Em 500 nm. All HPLC fractions were manually collected, dried, and further examined by MALDI TOF MS.

#### MALDI-TOF MS and MS/MS

Lyophilized glycan samples, either in native or derivatized forms (PA, AEAB, and fluorescein conjugates), were dissolved in HPLC grade water and subject to MALDI-TOF MS and MS/MS analyses on an Autoflex Speed instrument (1000 Hz Smartbeam-II laser, Bruker Daltonics) using 6-aza-2-thiothymine as a matrix (47). Calibration of the instrument was routinely performed using the Bruker Peptide Calibration Standard II to cover the MS range between 700 and 3200 Da. The detector voltage was normally set at 1977 V for MS and 2133 V for MS/MS; typically, 3000 shots from different regions of the sample spots were summed. Automatic measurements were conducted on HPLC-fractionated glycan samples (N2, tm5400, and cop1842) using the AutoXecute (https://www.cmu.edu/chemistry/facilities/cma/ instruments/manuals/flexcontrol-user-manual.pdf) of the control software (Bruker flexControl 3.4). To obtain MS/MS spectra, parent ions were fragmented by laserinduced dissociation without applying a collision gas (precursor ion selector was generally ±0.6%). For PA and AEABlabeled glycans, [M+H]+ ions were favored for laser-induced dissociation fragmentation, whereas for fluorescein conjugates [M+H-linker]+ ions, as "in-source degradation" products of the intact compounds, were fragmented because their MS/MS spectra presented the most informative fragments for structural annotation.

#### Growth, morphological, and behavioral analyses

Animal synchronization was made by treating gravid adults with standard hypochlorite-based procedure. Developmental speed was assessed by measuring the time between hatching and the onset of egg laying in animals maintained at 25 °C on regular nematode growth medium plates seeded with *E. coli* OP50. For each genotype, the growth time prior to behavioral assays was adjusted in order to test animals just after they started to lay their first eggs. Animal size,

postural, and locomotion parameters were obtained from videos recorded and analyzed as in Thapliyal et al. (37) using the Tierpsy Tracker v1.4 (https://github.com/ver228/tierpsytracker) (48). Fifteen assays per condition, each tracking a population of at least 20 animals, were recorded and the average value of selected postural and locomotion parameters extracted for each assay. Individual data points (dots) overlaid in the different bar graphs each represent the value derived from one assay. The "food-deprived" condition was acquired 3 h after food deprivation. Locomotion speed was normalized to the body length in order to compensate for variable animal sizes across genotypes. D'Agostino & Pearson test (p < 0.01) was used to test normality of distributions. Comparisons giving significant effects (p < 0.05) with ANOVAs were followed by Bonferroni post hoc tests. Dunn's test was used as nonparametric test whenever the normality assumption criterion was not fulfilled. All tests were two-tailed.

#### **Data availability**

Relevant MS and MS/MS data are converted to mzxml files and uploaded to GlycoPost: https://glycopost.glycosmos.org/entry/GPST000395.

Supporting information—This article contains supporting information (Supplementary Figures 1–7 and Supplementary Table 1).

Acknowledgments—We are thankful to the Japanese National Bioresource Project for providing *C. elegans* mutants; some strains were obtained from the CGC, which is funded by NIH Office of Research Infrastructure Programs (P40 OD010440). The authors acknowledge Dr Zuzanna Dutkiewicz and Dr Nicola Palmieri for their help with predicting putative glycoenzymes in nematode genomes, Licha Wortha for PCR verification of genotypes. We thank the BOKU Core Facility Mass Spectrometry for the use of the Autoflex Speed MALDI-TOF MS instrument and Dr Karin Hummel at the VetCore Proteomics for protein ID services.

Author contributions—J. K., F. W., S. T., E. A., H. G., S. K., D. M., M. R. S., D. P., T. L., and S. Y. methodology; S. T., E. A., D. M., C. U., and S. Y. visualization; S. T., K. P., D. A. G., and S. Y. formal analysis; D. M. and C. U. validation; K. P., I. B. H. W., and S. Y. data curation; D. A. G., I. B. H. W., and S. Y. supervision; I. B. H. W. and S. Y. conceptualization; K. P. and D. A. G. writing—review and editing; I. B. H. W. and S. Y. writing—original draft.

Funding and additional information—This work was supported by the Austrian Science Fund (FWF; grants P30021 to S. Y., P29466 to I. B. H. W. and P32572 to K. P.); The Swiss National Science Foundation (grant 310030\_197607 to D. A. G.).

Conflict of interest—The authors declare that they have no conflicts of interest with the contents of this article.

Abbreviations—The abbreviations used are: AEAB, 2-amino-N-(2-aminoethyl)benzamide; FUT, fucosyltransferase; GlcNAc, *N*-ace-tylglucosamine; MS/MS, tandem mass spectrometry; PA-MM, 2-aminopyridine labelled MM structure.



#### References

- Zhao, Y.-Y., Takahashi, M., Gu, J.-G., et al. (2008) Functional roles of Nglycans in cell signaling and cell adhesion in cancer. Cancer Sci. 99, 1304–1310
- Haltiwanger, R. S., and Lowe, J. B. (2004) Role of glycosylation in development. Annu. Rev. Biochem. 73, 491–537
- 3. Reily, C., Stewart, T. J., Renfrow, M. B., et al. (2019) Glycosylation in health and disease. Nat. Rev. Nephrol. 15, 346–366
- Yamaguchi, Y. (2002) Glycobiology of the synapse: the role of glycans in the formation, maturation, and modulation of synapses. *Biochim. Biophys.* Acta 1573, 369–376
- Liu, F.-T., and Stowell, S. R. (2023) The role of galectins in immunity and infection. Nat. Rev. Immunol. 23, 479–494
- Pinho, S. S., Alves, I., Gaifem, J., et al. (2023) Immune regulatory networks coordinated by glycans and glycan-binding proteins in autoimmunity and infection. Cell Mol. Immunol. 20, 1101–1113
- Paschinger, K., and Wilson, I. B. H. (2019) Comparisons of N-glycans across invertebrate phyla. *Parasitology* 146, 1733–1742
- 8. van Die, I., Gomord, V., Kooyman, F. N., et al. (1999) Core alpha1–3-fucose is a common modification of N-glycans in parasitic helminths and constitutes an important epitope for IgE from *Haemonchus contortus* infected sheep. *FEBS Lett.* **463**, 189–193
- Eckmair, B., Gao, C., Mehta, A. Y., et al. (2024) Recognition of highly branched N-glycans of the porcine whipworm by the immune system. Mol. Cell Proteomics 23, 100711
- Paschinger, K., Rendic, D., Lochnit, G., et al. (2004) Molecular basis of anti-horseradish peroxidase staining in *Caenorhabditis elegans*. J. Biol. Chem. 279, 49588–49598
- Paschinger, K., Staudacher, E., Stemmer, U., et al. (2005) Fucosyltransferase substrate specificity and the order of fucosylation in invertebrates. Glycobiology 15, 463–474
- Yan, S., Serna, S., Reichardt, N.-C., et al. (2013) Array-assisted characterization of a fucosyltransferase required for the biosynthesis of complex core modifications of nematode N-glycans. J. Biol. Chem. 288, 21015–21028
- Fabini, G., Freilinger, A., Altmann, F., et al. (2001) Identification of core alpha 1,3-fucosylated glycans and cloning of the requisite fucosyltransferase cDNA from *Drosophila melanogaster*. Potential basis of the neural anti-horseadish peroxidase epitope. J. Biol. Chem. 276, 28058–28067
- Boruah, B. M., Kadirvelraj, R., Liu, L., et al. (2020) Characterizing human α-1,6-fucosyltransferase (FUT8) substrate specificity and structural similarities with related fucosyltransferases. J. Biol. Chem. 295, 17027–17045
- Both, P., Sobczak, L., Breton, C., et al. (2011) Distantly related plant and nematode core α1,3-fucosyltransferases display similar trends in structure-function relationships. Glycobiology 21, 1401–1415
- 16. Yan, S., Bleuler-Martinez, S., Plaza, D. F., et al. (2012) Galactosylated fucose epitopes in nematodes: increased expression in a Caenorhabditis mutant associated with altered lectin sensitivity and occurrence in parasitic species. J. Biol. Chem. 287, 28276–28290
- Yan, S., Wilson, I. B. H., and Paschinger, K. (2015) Comparison of RP-HPLC modes to analyse the N-glycome of the free-living nematode Pristionchus pacificus. Electrophoresis 36, 1314–1329
- Jiménez-Castells, C., Vanbeselaere, J., Kohlhuber, S., et al. (2017) Gender and developmental specific N-glycomes of the porcine parasite Oesophagostomum dentatum. Biochim. Biophys. Acta Gen. Subj. 1861, 418–430
- Paschinger, K., and Wilson, I. B. H. (2015) Two types of galactosylated fucose motifs are present on N-glycans of *Haemonchus contortus*. Glycobiology 25, 585–590
- Martini, F., Eckmair, B., Štefanić, S., et al. (2019) Highly modified and immunoactive N-glycans of the canine heartworm. Nat. Commun. 10, 75
- Kawar, Z., Karaveg, K., Moremen, K. W., et al. (2001) Insect cells encode a class II alpha-mannosidase with unique properties. J. Biol. Chem. 276, 16335–16340

- Nemčovičová, I., Šesták, S., Rendić, D., et al. (2013) Characterisation of class I and II α-mannosidases from *Drosophila melanogaster*. Glycoconj J. 30, 899–909
- Paschinger, K., Hackl, M., Gutternigg, M., et al. (2006) A deletion in the golgi alpha-mannosidase II gene of *Caenorhabditis elegans* results in unexpected non-wild-type N-glycan structures. *J. Biol. Chem.* 281, 28265–28277
- 24. Tomiya, N., Lee, Y. C., Yoshida, T., et al. (1991) Calculated two-dimensional sugar map of pyridylaminated oligosaccharides: elucidation of the jack bean alpha-mannosidase digestion pathway of Man9GlcNAc2. Anal Biochem. 193, 90–100
- 25. Yan, S., Vanbeselaere, J., Jin, C., et al. (2018) Core Richness of N-glycans of Caenorhabditis elegans: a case study on chemical and enzymatic release. Anal Chem. 90, 928–935
- Wilson, I. B. H., Yan, S., Jin, C., et al. (2023) Increasing Complexity of the N-glycome during Caenorhabditis development. Mol. Cell Proteomics 22, 100505
- Paschinger, K., Wöls, F., Yan, S., et al. (2023) N-glycan antennal modifications are altered in *Caenorhabditis elegans* lacking the HEX-4 N-acetylgalactosamine-specific hexosaminidase. J. Biol. Chem. 299, 103053
- Barrows, B. D., Haslam, S. M., Bischof, L. J., et al. (2007) Resistance to Bacillus thuringiensis toxin in Caenorhabditis elegans from loss of fucose. J. Biol. Chem. 282, 3302–3311
- 29. Titz, A., Butschi, A., Henrissat, B., et al. (2009) Molecular basis for galactosylation of core fucose residues in invertebrates: identification of Caenorhabditis elegans N-glycan core alpha1,6-fucoside beta1,4-galactosyltransferase GALT-1 as a member of a novel glycosyltransferase family. J. Biol. Chem. 284, 36223–36233
- Yan, S., Jin, C., Wilson, I. B. H., et al. (2015) Comparisons of Caenorhabditis fucosyltransferase mutants reveal a multiplicity of isomeric Nglycan structures. J. Proteome Res. 14, 5291–5305
- 31. Yan, S., Brecker, L., Jin, C., et al. (2015) Bisecting galactose as a feature of N-glycans of wild-type and mutant *Caenorhabditis elegans*. Mol. Cell Proteomics 14, 2111–2125
- 32. Paschinger, K., Yan, S., Pohl, N. L., et al. (2021) 5.02 glycobiology of *Caenorhabditis elegans*. In: Barchi, J. J., ed. *Comprehensive Glycoscience*, 2nd Ed., Elsevier, Oxford: 36–54
- **33.** Paschinger, K., Yan, S., and Wilson, I. B. H. (2019) N-Glycomic complexity in anatomical simplicity: *Caenorhabditis elegans* as a non-model nematode? *Front. Mol. Biosci.* **6**, 9
- 34. Yang, Q., and Wang, L.-X. (2016) Mammalian α-1,6-fucosyltransferase (FUT8) is the sole enzyme responsible for the N-acetylglucosaminyltransferase I-independent core fucosylation of high-mannose N-glycans. J. Biol. Chem. 291, 11064–11071
- 35. Zhu, F., Li, D., and Chen, K. (2019) Structures and functions of invertebrate glycosylation. *Open Biol.* 9, 180232
- Flavell, S. W., Raizen, D. M., and You, Y.-J. (2020) Behavioral states. *Genetics* 216, 315–332
- 37. Thapliyal, S., Beets, I., and Glauser, D. A. (2023) Multisite regulation integrates multimodal context in sensory circuits to control persistent behavioral states in *C. elegans. Nat. Commun.* 14, 3052
- Herscovics, A. (1999) Importance of glycosidases in mammalian glycoprotein biosynthesis. *Biochim. Biophys. Acta* 1473, 96–107
- **39.** Suzuki, T., Hara, I., Nakano, M., *et al.* (2006) Man2C1, an alpha-mannosidase, is involved in the trimming of free oligosaccharides in the cytosol. *Biochem. J.* **400**, 33–41
- Park, C., Meng, L., Stanton, L. H., et al. (2005) Characterization of a human core-specific lysosomal {alpha}1,6-mannosidase involved in Nglycan catabolism. J. Biol. Chem. 280, 37204–37216
- Wilson, I. B. H., and Paschinger, K. (2016) Sweet secrets of a therapeutic worm: mass-spectrometric N-glycomic analysis of *Trichuris suis. Anal Bioanal. Chem.* 408, 461–471
- Roberts, B., Antonopoulos, A., Haslam, S. M., et al. (2013) Novel expression of Haemonchus contortus vaccine candidate aminopeptidase H11 using the free-living nematode Caenorhabditis elegans. Vet. Res. 44, 111



- 43. Rahman, M., Ramirez-Suarez, N. J., Diaz-Balzac, C. A., et al. (2022) Specific N-glycans regulate an extracellular adhesion complex during somatosensory dendrite patterning. EMBO Rep. 23, e54163
- 44. Kubota, Y., Sano, M., Goda, S., et al. (2006) The conserved oligomeric Golgi complex acts in organ morphogenesis via glycosylation of an ADAM protease in C. elegans. Development 133, 263-273
- 45. Lefeber, D. J., Freeze, H. H., Steet, R., et al. (2022) Essentials of glycobiology. In Congenital Disorders of Glycosylation, 4th Ed., Cold Spring Harbor Laboratory Press. Cold Spring Harbor, NY
- 46. Dragosits, M., Yan, S., Razzazi-Fazeli, E., et al. (2015) Enzymatic properties and subtle differences in the substrate specificity of phylogenetically
- distinct invertebrate N-glycan processing hexosaminidases. Glycobiology **25**, 448–464
- 47. Paschinger, K., Razzazi-Fazeli, E., Furukawa, K., et al. (2011) Presence of galactosylated core fucose on N-glycans in the planaria Dugesia japonica. J. Mass Spectrom. 46, 561-567
- 48. Javer, A., Currie, M., Lee, C. W., et al. (2018) An open-source platform for analyzing and sharing worm-behavior data. Nat. Methods 15, 645-646
- 49. Varki, A., Cummings, R. D., Aebi, M., et al. (2015) Symbol Nomenclature for graphical representations of glycans. Glycobiology 25, 1323-1324

